WEIGHT OPTIMIZATION FOR HYBRID, MULTI-SCALE CNT/FIBRE REINFORCED COMPOSITE LAMINATES

by

Shivaan Anashpaul
214502323

Submitted in fulfillment of the requirements for the degree of
Master of Science in Civil Engineering

School of Civil Engineering, Surveying and Construction
University of KwaZulu-Natal
Durban

January 2021

Supervisor: Prof Georgios A. Drosopoulos

PREFACE

The research presented in this dissertation was conducted from the Civil Engineering Department, at the University of KwaZulu-Natal, from February 2020 to January 2021, under the supervision of Prof. Georgios A Drosopoulos

As the candidate's Supervisor I agree to the submission of this thesis

…………………………..……signed at…Preston, UK……………., on……27/01/2021……

DECLARATION - PLAGIARISM

I, **Shivaan Anashpaul**, declare that

1. The research reported in this thesis, except where otherwise indicated, is my original research.

2. This thesis has not been submitted for any degree or examination at any other university.

3. This thesis does not contain other persons' data, pictures, graphs, or other information, unless specifically acknowledged as being sourced from other persons.

4. This thesis does not contain other persons' writing, unless specifically acknowledged as being sourced from other researchers. Where other written sources have been quoted, then:

   a. Their words have been re-written, but the general information attributed to them has been referenced

   b. Where their exact words have been used, then their writing has been placed in italics and inside quotation marks and referenced.

5. This thesis does not contain text, graphics or tables copied and pasted from the Internet, unless specifically acknowledged, and the source being detailed in the thesis and in the References sections.

Signed

……………………………………………

Shivaan Anashpaul

ACKNOWLEDGEMENTS

I would like to express gratitude and appreciation to the following people:

- My supervisor, Prof. Georgios Drosopoulos, for his dedication and expert guidance throughout this research and inspiring me on the topic of composites, programming, and finite element analysis.
- My co-supervisor, Prof Sarp Adali, for providing expert advice with composite structures.
- Friends and colleagues, for motivation to complete this dissertation.
- Family members, aunts and uncles for their support and encouragement.
- Dr. Mayshree Singh, for inspiration and support throughout this degree.
- Parents and grandparents, for everything.

ABSTRACT

In this study, an investigation on an optimal lightweight design of a 3-phase CNT/fibre reinforced nanocomposite plate was conducted, subject to a frequency constraint. The design variables for the optimization process are, fibre volume fraction, CNT weight fraction, fibre stacking angle, and layer thickness ratio. A literature study was carried out to set the foundation to the key concepts and methods used to carry out the optimization process. The effective material properties were obtained using a 2-step process which were formulated with Halpin-Tsai equations and fibre micromechanics. The solution for the natural vibration of composite laminates was carried out using the Ritz method and Classical Laminate Plate Theories (CLPT). For the design of the weight optimization of the composite plate, the Sequential Quadratic Programming (SQP) algorithm was adopted, using MATLAB, to carry out the non-linear optimization problems with the design constraints. A verification of the vibration and optimization methods was conducted using FEM and ANSYS. Five optimization problems were defined to assess the parameters which affect the weight optimization. The solution to the optimization problems reached an optimal fibre stacking angle of 45° for square laminates and increasing towards 90° for rectangular laminates with aspect ratios greater than 1, up to 2. The use of CNTs in the composite plate was highlighted where the addition of CNTs have improved the minimum weight design for higher non-dimensional frequencies from 1.75 up to 2.5. An optimum design efficiency was achieved, showing a 52.7% weight improvement of the 3-phase laminate with the design variables assigned. Efficient material utilization was implemented optimally, which allocated higher amounts of reinforcement materials, CNTs and fibre, in the exterior layers. The weight optimization using non-uniform layer thicknesses resulted in the exterior layers to have a higher thickness than the interior layers, which contributed to an efficient minimum weight design.

TABLE OF CONTENTS

PREFACE .... **II**

DECLARATION - PLAGIARISM .... **III**

ACKNOWLEDGEMENTS .... **IV**

ABSTRACT .... **V**

TABLE OF CONTENTS .... **VI**

LIST OF FIGURES .... **IX**

LIST OF TABLES .... **XI**

LIST OF ABBREVIATIONS .... **XIII**

CHAPTER 1 - INTRODUCTION **1**

1.1 BACKGROUND TO THE STUDY 1
1.2 STATE OF ART 2
1.3 RESEARCH QUESTION 3
1.4 AIMS 3
1.5 OBJECTIVES 3
1.6 STRUCTURE OF THE DISSERTATION 4

CHAPTER 2 - LITERATURE REVIEW **5**

2.1 INTRODUCTION 5
2.2 NANOTECHNOLOGY IN AFRICA 5
2.3 NANOMATERIALS IN ENGINEERING 6
2.3.1 Nanomaterials in Civil Engineering 6
2.3.2 Nanomaterials in Aerospace and other Engineering Industries 7
2.4 PROPERTIES OF CARBON NANOTUBES 8
2.5 FIBRE REINFORCED COMPOSITES (FRC) 11
2.5.1 The Development of Composite Materials 11
2.5.2 Constituents of FRCs 11
2.5.3 Classification of Composite Materials 12
2.6 MICRO-SCALE MODELLING 14
2.6.1 Two-phase CNT reinforced matrix Halpin-Tsai equation formulation 16
2.6.2 Three-phase fibre/CNT reinforced matrix composite 17
2.7 VIBRATION OF COMPOSITE STRUCTURES 17
2.8 OPTIMIZATION OF COMPOSITE STRUCTURES 19
2.8.1 Optimization Algorithms 19
2.8.2 Optimal Composite Design 21
2.9 FINITE ELEMENT ANALYSIS (FEA) 23

2.10 SUMMARY 24

CHAPTER 3 - METHODOLOGY 25

3.1 INTRODUCTION 25
3.2 SEQUENTIAL QUADRATIC PROGRAMMING (SQP) 25
3.3 COMPOSITE MODELLING 26
3.4 VIBRATION OF LAMINATE COMPOSITES 26
3.4 1 Formulation of the Analytical Approach 26
3.4.2 Formulation of the Non-Dimensional Solution 28
3.5 FORMULATION OF THE OPTIMIZATION PROBLEMS 29
3.5.1 Problem 1: 2-Phase Uniform Layer Thickness and Non-Uniform Distribution of Reinforcement Material (Design variable: V_F) 30
3.5.2 Problem 2: 3-Phase Uniform Layer Thickness and Non-Uniform Distribution of Reinforcement Material (Design variable: V_F) 31
3.5.3 Problem 3: 3-Phase Uniform Layer Thickness and Non-Uniform Distribution of Reinforcement Material (Design variables: V_F and W_{CNT}) 32
3.5.4 Problem 4: 3-Phase Uniform Layer Thickness and Non-Uniform Distribution of Reinforcement Material (Design variables: V_F, W_{CNT}, fibre angle) 33
3.5.5 Problem 5: 3-Phase Non-Uniform Layer Thickness and Non-Uniform Distribution of Reinforcement Material (Design variables: V_F, W_{CNT}, fibre angle, thickness ratio) 34
3.6. VERIFICATION 35
3.7 SUMMARY 38

CHAPTER 4 - RESULTS AND DISCUSSION 39

4.1 INTRODUCTION 39
4.2 ANALYSIS RESULTS 39
4.3 OPTIMIZATION RESULTS 43
4.3.1 Problem 1: 2-Phase Uniform Layer Thickness and Non-Uniform Distribution of Reinforcement Material (Design variable: V_F) 43
4.3.2 Problem 2: 3-Phase Uniform Layer Thickness and Non-Uniform Distribution of Reinforcement Material (Design variable: V_F) 44
4.3.3 Problem 3: 3-Phase Uniform Layer Thickness and Non-Uniform Distribution of Reinforcement Material (Design variables: V_F and W_{CNT}) 46
4.3.4 Problem 4: 3-Phase Uniform Layer Thickness and Non-Uniform Distribution of Reinforcement Material (Design variables: V_F, W_{CNT}, fibre angle) 53
4.3.5 Problem 5: 3-Phase Non-Uniform Layer Thickness and Non-Uniform Distribution of Reinforcement Material (Design variables: V_F, W_{CNT}, fibre angle, thickness ratio) 55
4.4 SUMMARY 57

CHAPTER 5 - CONCLUSION & RECOMMENDATIONS 58

5.1 CONCLUSION 58

5.2 RECOMMENDATIONS AND FUTURE WORK 60

REFERENCES 61

APPENDIX A - EFFECTIVE PROPERTIES 68

APPENDIX B – ANSYS RESULTS 69

LIST OF FIGURES

Figure 2-1:Carbon nanotube publications with the keywords aerospace and aircraft, between the years 2000 and 2013 (Source: Gohardani et al. (2014)) 7
Figure 2-2: Graphene: The building blocks of carbon allotropes (Source:Garg et al. (2014)) 8
Figure 2-3 (A) Single-Wall CNT (SWCNT), (B) Multi-Wall CNT (MWCNT) (Source: Vidu et al. (2014)) 9
Figure 2-4: Roll-up vector defining the structure of carbon nanotubes (Source: Kalamkarov et al. (2006)) 10
Figure 2-5: Structure of single-wall SWCNT with different chiral angles between 0° and 30° (Source: Sanchez et al. (2005)) 10
Figure 2-6: Composite materials: (a) Based on matrix material; (b) Based on reinforcement material (Source: Yang et al. (2012)) 13
Figure 2-7: Dispersion of CNTs in polymer matrix, thereafter fibres in CNT/polymer nanocomposite (Source: Rafiee et al. (2018)) 15
Figure 2-8: Design optimization process (Source: Maalawi (2018)) 19
Figure 2-9: The flowchart of the SQP technique (Source: (Morshed and Asgharpour, 2014)) .. 20
Figure 3-1: Coordinate system and layer numbering used for a laminate plate 26
Figure 3-2: Geometry of the composite plate 29
Figure 3-3: ANSYS model of the simply supported composite plate 35
Figure 3-4: Verification of the weight optimization methodology 37
Figure 4-1: Non-dimensional weight vs fibre angle for a composite plate showing the addition of CNT reinforcement incrementally (Left: 30%fibre+0%CNT; Centre: 30%fibre+1%CNT; Right: 30%fibre+5%CNT) 40
Figure 4-2:Non-dimensional frequency vs fibre angle for a composite plate showing the addition of CNT reinforcement incrementally (Left: 30%fibre+0%CNT; Centre: 30%fibre+1%CNT; Right: 30%fibre+5%CNT) 41
Figure 4-3: Optimal Non-Dimensional weight vs Fibre stacking angle for a 2-Phase laminate H=0.01; 0≤Vf≤0.6; Aspect ratio= a/b; f=1.3 43
Figure 4-4: Optimal Non-dimensional weight vs Fibre stacking angle for a 3-Phase laminate H=0.01; $0 \leq V_f \leq 0.6$; Aspect ratio= a/b; f=1.3; W_{CNT}=1%(LEFT) ; W_{CNT}=2%(RIGHT) 44
Figure 4-5: Surface plots for the 3-Phase square laminate showing the volume fraction and weight fraction of CNT and glass fibres in the surface layers; H=0.01; $0 \leq V_{fi} \leq 0.6$; $0 \leq W_{CNTi} \leq 0.05$; a/b= 1; f=1.75 46
Figure 4-6: Fibre and CNT reinforcement per layer versus non-dimensional frequency 47

Figure 4-7: Graphs showing the optimized quantities for the specified frequency constraints for an 8-layered laminate subject to H=0.01; $0 \leq V_{fi} \leq 0.6$; $0 \leq W_{CNTi} \leq 0.05$; a/b= 1; θ=45°................48
Figure 4-8: Optimum Non-dimensional weight vs %Vol. Fibre Content for 3-phase laminate .49
Figure 4-9: Optimum Minimum Weight vs Different Stacking sequences for 2-Phase and 3-Phase laminate; subject to H=0.01; $0 \leq V_{fi} \leq 0.6$; $0 \leq W_{CNTi} \leq 0.05$; W_{CNTmax}=1.25%; a/b=1; f=1.75.........51
Figure 4-10: Surface plots for the 3-Phase square laminate showing the total weight % of CNT and the optimal fibre angle in all layers; subject to H=0.01; $0 \leq V_{fi} \leq 0.6$; $0 \leq W_{CNTi} \leq 0.05$; W_{CNTmax}=as shown; a/b= 1; f=1.75...52

LIST OF TABLES

Table 2-1: Top 10 applications of nanotechnology in developing countries (after United Nations. Economic Commission for Africa (2020)) 5

Table 2-2: Potentials of CNTs in aeronautics and astronautics (after Gohardani et al. (2014)) .. 7

Table 2-3: Representative properties of nanomaterials and other common materials in composites (after (Gong, 2018) and (Tserpes and Silvestre, 2014)) 11

Table 2-4: Effective scales of involved parameters and modelling methods at each scale (after Rafiee and Eskandariyun (2019)) 14

Table 2-5:Comparison of SQP, GA, SA and PSO optimization algorithms (after Aktemur and Gusseinov (2017) 20

Table 3-1: Comparison of numerical results for a 3-layered SSSS square laminate 36

Table 3-2: Material properties 36

Table 3-3: Comparison of Numerical results with commercial software for 3-ply CNT/Fibre reinforced laminate 37

Table 3-4: Comparison of Numerical results with commercial software for 8-layer CNT/Fibre reinforced laminate 38

Table 4-1:Non-dimensional quantities showing results for CNT and fibre assigned explicitly .42

Table 4-2: Optimal fibre angle and optimal Non-dimensional weight for 2-Phase laminate. H=0.01; $0 \le V_f \le 0.6$; Aspect ratio= a/b; f=1.3 43

Table 4-3:Optimal fibre angle and optimal Non-dimensional weight for 3-Phase laminate. H=0.01; $0 \le V_f \le 0.6$; Aspect ratio= a/b; f=1.3; W_{CNT}=1% 45

Table 4-4:Optimal fibre angle and optimal Non-dimensional weight for 3-Phase laminate. H=0.01; $0 \le V_f \le 0.6$; Aspect ratio= a/b; f=1.3; W_{CNT}=2% 45

Table 4-5: Detailed solution to the diagrams in Figure 4-8 50

Table 4-6: Minimum weight design for 2-Phase and 3-Phase laminate with 8-layeres subject to H=0.01; $0 \le V_{fi} \le 0.6$; $0 \le W_{CNTi} \le 0.05$; W_{CNTmax}=1.25%; a/b=1; f=1.75 for different stacking sequences 51

Table 4-7: Minimum weight design for 3-Phase laminate with 8-layers subject to 3 design variables H=0.01; $0 \le V_{fi} \le 0.6$; $0 \le W_{CNTi} \le 0.05$; W_{CNTmax}=1.25%; $-90 \le \theta \le +90$; a/b=1 54

Table 4-8: Optimal fibre angle and optimal Non-dimensional weight for 3-Phase laminate. H=0.01; $0 \le V_f \le 0.6$; $0 \le W_{CNTi} \le 0.05$; W_{CNTmax}=1%; $-90 \le \theta \le +90$; Aspect ratio= a/b; f=1.3 54

Table 4-9: Minimum weight design for 3-Phase laminate with 8-layers subject to 4 design variables, H=0.01; $0 \le V_{fi} \le 0.6$; $0 \le W_{CNTi} \le 0.05$; W_{CNTmax}=1.25%; $-90 \le \theta \le +90$; $0.01 \le h/H \le 0.15$; a/b=1; $\sum_{i=1}^{8} \frac{h_i}{H} = 1$ 56

Table A-0-1: Effective layer material properties 68
Table B-0-1: Optimal weight quantities determined using ANSYS 69
Table B-0-2: Optimal Frequency quantities determined using ANSYS 70

LIST OF ABBREVIATIONS

aeDE	–	adaptive elitist Differential Evolution
ANN	–	Artificial Neural Networks
ANSYS	–	Analysis System (Finite Element Analysis Software)
CF	–	Carbon Fibre
CLPT	–	Classical Laminate Plate Theory
CNF	–	Carbon Nanofibres
CNT	–	Carbon Nanotube
CVD	–	Chemical Vapour Deposition
DSC	–	Discrete Single convolution
E	–	Youngs Modulus
ESL	–	Equivalent Single Layer
FDM	–	Feasible direction method
FEA	–	Finite Element Analysis
FEM	–	Finite Element Method
FRC	–	Fibre Reinforced Composite
FRP	–	Fibre Reinforced Polymer
G	–	Shear Modulus
GA	–	Genetic Algorithm
GPa	–	Gigapascal
HMM	–	Hierarchical multi-scale modelling
LOA	–	Layer-wise Optimization Algorithm
MPa	–	Megapascal
MWCNT	–	Multi Wall Carbon nanotube
NSGA-II	–	non-dominated sorting genetic algorithm
PSO	–	Particle Swarm Algorithm

PRC	–	Particle Reinforced Composites
RVE	–	Representative Volume Elements
SA	–	Simulated Annealing
SSSS	–	Simply Supported boundary condition
SWCNT	–	Single Wall Carbon nanotube
SQP	–	Sequential Quadratic Programming
TPa	–	Tera Pascal
UNECA	–	United Nations. Economic Commission for Africa
μm	–	Micrometer
nm	–	Nano-meters
ν	–	Poisson's ratio
V	–	Volume
W	–	Weight
ω	–	omega
θ	–	theta
°	–	degree

CHAPTER 1 - INTRODUCTION

1.1 Background to the Study

Weight reduction and development of advanced composite materials have shown potential in composite engineering as there has been several engineering applications which can benefit by the use of extraordinary materials. Composite engineering focuses on utilizing materials effectively to meet the desired needs. This study investigates the lightweight design of an advanced composite laminate plate by the use of nanotechnology and optimization methods to optimize the materials and parameters while achieving the desired objective.

Over the years, scientists and engineers have aimed to incorporate sustainable solutions into research and development, which promotes helping the environment and helping to grow society. The three pillars of sustainable development are social development, environmental development, and economic development, and these are known to be the key principles which uphold the values and ensures that sustainable development is met for all facets of life on this planet.

"Sustainable development is development that meets the needs of the present without compromising the ability of future generations to meet their own needs" - (Bruntland, 1987)

In the engineering industry, over the years, sustainability has been strived for by the efficient use of raw materials in engineering applications. The development of structures and materials from the efficient use of raw materials have led to new innovations and more enhanced composite structures and materials being developed. Composite materials have shown enhanced properties, which have been utilized in many high-performance applications. In modern day applications, such as in aircrafts, spacecrafts, boats and motor vehicles, composite materials have been tailored for their application and has helped reduced the amount of steel and other raw materials used. According to Jones (1998), some of the properties which are enhanced by forming composite materials are:

- Attractiveness
- Corrosion resistance
- Stiffness
- Temperature-dependant behaviour
- Thermal conductivity
- Wear resistance
- Acoustic insulation
- Fatigue life
- Strength
- Thermal insulation
- Weight

Efficient and optimized use of materials and resourced is employed to ensure that there are sufficient materials being utilized, without excessive wastage and performance depreciation, which results in lower costs and optimal performances. However, the formulation of advanced composite materials and composite structures have now shown to be the future for modern day science and technological applications hence a greater need for improved optimization methods and materials. Nanotechnology has been researched extensively in the last decades and has then been widely used in the engineering industry. After being discovered in 1991 by Iijima (1991), nanomaterials such as carbon nanotubes (CNTs) and graphene have been shown to be suitable candidates as reinforcement alternatives in composite materials and laminates (Duc et al., 2017, Mehar et al., 2017). The use of nanomaterials in composites enhances its strength and reduces the overall weight of the structure. Such advanced composites are highly suitable for vibration, buckling and bending problems and has a high potential in many application which incorporates lightweight and versatile designs (Demiroglu et al., 2017, Nasrollahzadeh et al., 2019). This study strives to fully utilise the properties of CNTs in a multiphase multiscale nanocomposite design, by means of optimization techniques and vibration analysis methods.

1.2 State of art

In recent times, the lightweight design of structures has been greatly improved by using engineered materials and updated manufacturing processes and systems. Currently, with composite materials, carbon-based materials have been integrated in aerospace and aircraft engineering with applications such as carbon fibre panels on airplanes and graphene and CNT coating for lightning protection. According to Gohardani et al. (2014), several patents have been issued for CNTs in aerospace applications. The suitability of new materials such as CNTs is possible through extensive research and testing through computational mechanics and numerical solutions.

In the present material engineering research, micromechanical modelling and simulations provide a higher understanding of new materials and composites, and their properties for relevant applications. Current micromechanics techniques help model failure systems in a structure using Representative Volume Elements (RVE) (Mccarthy and Vaughan, 2015). Natural vibration problems and modelling of structures are possible through state-of-the-art computer programs such as ANSYS, Abaqus and MATLAB, where optimization techniques suitable for engineering applications are being implemented.

1.3 Research Question

What effect does the parameters and design variables of the composite plate have on achieving an optimum minimum weight design?

1.4 Aims

The aims of this study are to:

- Research and understand the properties of carbon nanotubes and fibre reinforcement in a composite plate,
- Successfully model the composite plate with effective material properties using micromechanics and Halpin-Tsai equations.
- Investigate the vibration behaviour of the CNT/fibre reinforced composite plate with different amounts of CNT and fibre and provide solutions for the optimization of the weight of the reinforced laminate.
- Evaluate results from numerical investigations and draw meaningful conclusions as well as provide recommendations.

1.5 Objectives

- Review on past literature to develop an understanding of the vibration behaviour of composites and acquire material properties.
- Obtain effective material properties for the composite plate using micromechanics and MATLAB software.
- Build numerical models using MATLAB software.
- Test MATLAB code and compare results with similar investigations from past literature.
- Use analytical methods to carry out the optimization of the weight of the composite plate according to the amount of CNT and fibre present, subject to different frequency constraints.
- Investigate the vibration behaviour by changing the parameters and material quantities of the composite plate.
- Evaluate and analyse results by means of graphs and figures and develop relationships which help draw conclusions for the study.
- Provide recommendations for the materials used and different conditions for the composite plate which can be used for future research.

1.6 Structure of the Dissertation

This dissertation comprises of five chapters followed by a list of references and appendices. These chapters give an overview on nanotechnology and the implementation of nanomaterials for an optimal weight design of a composite plate. The breakdown for the chapters to follow are provided below.

- Chapter 1 - provides the background information and the state of art of this research. The research question, aims and objectives are defined which form as the purpose of the study.

- Chapter 2 - reviews past literature on the topic to obtain greater knowledge on nanomaterials, modelling of composite structures, and optimization of composites structures under vibration.

- Chapter 3 - entails a methodology which shows the derivation of the micromechanical equations used for the homogenisation of the 2 and 3-phase materials and the formulation for the different optimization problems is presented. This includes the design constraints and the design variables used in each optimization problem. The rationale for this chapter was based on plate vibration theories and optimization methods used in past literature. The verification of the vibration and optimization approach was also conducted.

- Chapter 4 - this chapter presents the results for the optimization problems which were defined in the methodology. It provides a discussion of the results with detailed descriptions for each optimization problem and highlighting the innovation of this study by using carbon nanotubes.

- Chapter 5 - presents the final conclusions of the study. The key findings from the optimization problems and the design parameters of the composite plate are addressed. The research question is answered, and the aims and objectives are discussed with reference to the findings from the study.

CHAPTER 2 - LITERATURE REVIEW

2.1 Introduction

This chapter presents the theoretical background and key concepts for this study. Important parameters are reviewed which help establish the methodology in Chapter 3. Nanotechnology and their applications are introduced, followed by material modelling and vibration of composite structures. Several optimization methods are reviewed and analysis techniques using finite element analysis and the finite element method.

2.2 Nanotechnology in Africa

Nanotechnology is one of the fields in science and technology which is still developing in Africa and has gained some traction in countries like South Africa, Egypt, Tunisia, Ethiopia, and the United Republic of Tanzania. Innovation through nanotechnology has helped develop and provide solutions to some of the current challenges being faced in Africa. African innovations such as nanofilters for water purification to nanocatalysts and nanosensors brought much attention to researchers and has enabled further research and development to be pursued in African countries (UN.ECA, 2020).

According to Salamanca-Buentello et al. (2005), the impact of nanotechnology on sustainable development can be assessed by comparing the leading nanotechnology applications to the UN Millennium Development Goals. Prior to this, the Economic Commission of Africa (UN.ECA, 2020) identified the primary and secondary sustainable development goals on which the top 10 nanotechnology applications would have a significant impact on. Table 2-1 highlights the top 10 applications of nanotechnology which has the potential of generating business opportunities and providing economic growth to developing countries.

Table 2-1: Top 10 applications of nanotechnology in developing countries (after United Nations. Economic Commission for Africa (2020))

Nanotechnology applications	Primary Goal	Secondary Goal
1.Energy storage,production, and conversion	Energy	Infrastructure/industrialization
2.Agricultural productivity enhancement	Zero hunger	End poverty in all forms
3.Water treatment and remediation	Water and sanitation	Health
4.Disease diagnosis and screening	Health	Infrastructure/industrialization
5.Drug delivery systems	Health	Infrastructure/industrialization
6.Food processing and storage	Zero hunger	Climate change
7.Air pollution and remediation	Cities	Health
8.Construction	Infrastructure/industrialization	Cities
9.Health monitoring	Health	Cities
10.Vector and pest detection and control	Health	Cities

2.3 Nanomaterials in Engineering

Research and development of nanomaterials have increased and improved through the years by means of updated scientific equipment and innovative technological solutions. Since the discovery of the extraordinary carbon based materials by Iijima (1991), nanomaterials such as graphene and carbon nanotubes have sparked interests in many engineering applications and industries. Nanotechnology refers to the restructuring and controlling of matter based on particle sizes from 0.1-100 nanometers (nm). This enables more flexibility of adapting the nanomaterial properties to suit the application for the material and to ensure that sustainable engineering solutions are acquired (Rao et al., 2015).

2.3.1 Nanomaterials in Civil Engineering

Considering the potential of such nanomaterials and its versatility, there have been several research topics in the different industries where nanotechnology and nanomaterials, such as graphene and carbon nanotubes, have been extensively researched and favoured for present and future innovative applications. A review study by Hossain and Rameeja (2015) showed that there are many beneficial uses of nanotechnology in the civil engineering industry.

Concrete, being one of the most common construction materials, has been used in almost every construction works. In the construction industry, the significant impact of concrete can be seen by it occupying up to 70 percent of the materials by volume of most structures. Research and development have been carried out to address the disadvantages of using cement and to reduce the amount of cement being incorporated in concrete by means of nanotechnology. This also involves minimising crack propagation and to increase the lifespan and durability of concrete (Rao et al., 2015). Steel, also being one of the crucial materials used in construction, has its challenges and disadvantages under fatigue, corrosion, and failure. Through nanotechnology and incorporating copper nano particles into steel, studies have shown that fatigue, caused by cyclic loading can be reduced. Fire protection, and corrosion resistance have also shown promising results with nanotechnology by means of spray-on-cementitious coating processes (Hossain and Rameeja, 2015).

According to Sanchez and Sobolev (2010), applications and advances of nanotechnology in the building environment has not been very smooth when introducing them on a commercial scale. This is due to; cost implications, quality, and quantity of nanomaterials from proper dispersion of nanoscale additives in the composite, and the manufacturing techniques of obtaining materials like graphene and carbon nanotubes.

2.3.2 Nanomaterials in Aerospace and other Engineering Industries

In certain industries, like the biomedical, electronic and optical industries, carbon-based nanomaterials have been favoured compared to other organic materials and have been used in a number of applications (Wang and Blau, 2007). Shown in Figure 2-1, the trend and research interests of CNTs have grown since the discovery of this extraordinary material and the number of applications in the aircraft and aerospace industry have increased as engineers and scientists aim to fully utilise the extraordinary properties of CNTs.

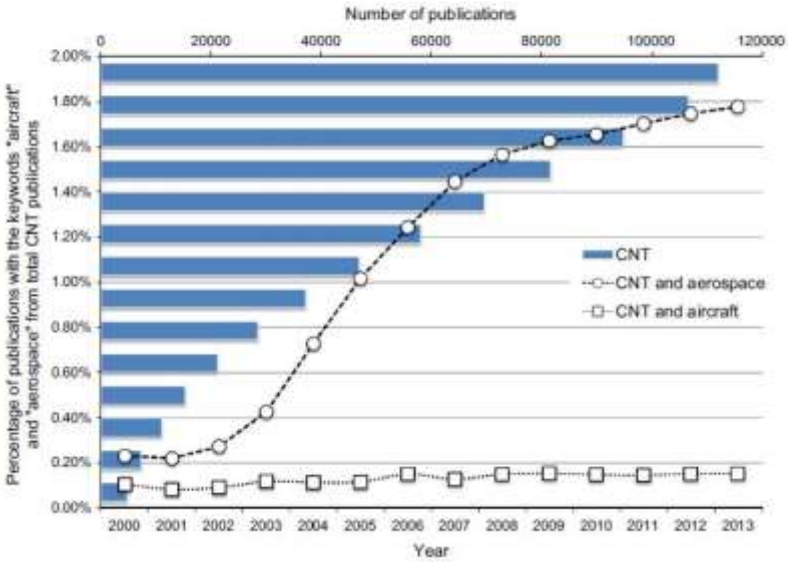

Figure 2-1:Carbon nanotube publications with the keywords aerospace and aircraft, between the years 2000 and 2013 (Source: Gohardani et al. (2014))

According to Uppal (2020), the current potential of CNTs in aircraft and aerospace is vast as manufacturers strive to make components lighter, stronger, and tougher with a higher life span. Nanomaterials are utilized in the aerospace industry so that they can deliver multi-functional properties like lightweight conductive composites and exhibit improved mechanical and electrical performances. Currently, research and development of nanomaterials in aerospace is focused mainly on structural reinforcement of composites materials to be used as components in these aircrafts. This allows for development of modern high-performance and multi-functional aircrafts which are more fuel efficient and cost-efficient due to the weight reduction and improved structural components. A summary of potential and prospective implementation of CNTs on next generation aircraft and space vehicles is shown in Table 2-2.

Table 2-2: Potentials of CNTs in aeronautics and astronautics (after Gohardani et al. (2014))

Aeronautics	Astronautics
Commercial aircrafts : Airframe, wiring, aircraft icing, propulsion, lightning protection, electromagnetic interference shielding, sensing, safety	Space elevator
Military aircrafts : stealth, aircraft icing	Space propulsion
Rotorcrafts : structural damping, structural monitoring, icing on rotorshaft	Satellites and spacecrafts
UAVs and MAVs : electric UAVs, mitigation of aircraft icing on UAVs	

2.4 Properties of Carbon Nanotubes

Carbon is one of the elements known to have many allotropes due to it having many hybridization states. Graphene being among the many allotropes of carbon makes up a 2-dimensional, single-layered nanosheet and is formed by hexagonal lattice structure bonded by sp2 hydrogen bonds (Tserpes and Silvestre, 2014). It is known to be the building block to all the other allotropes of carbon which each have their own dimensions and distinctive properties. Shown in Figure 2-2, the different allotropes of carbon where graphite is formed by stacking of graphene nanosheets, fullerenes or bucky balls formed by wrapping graphene nanosheets, and carbon nanotubes formed by rolling of the graphene nanosheets.

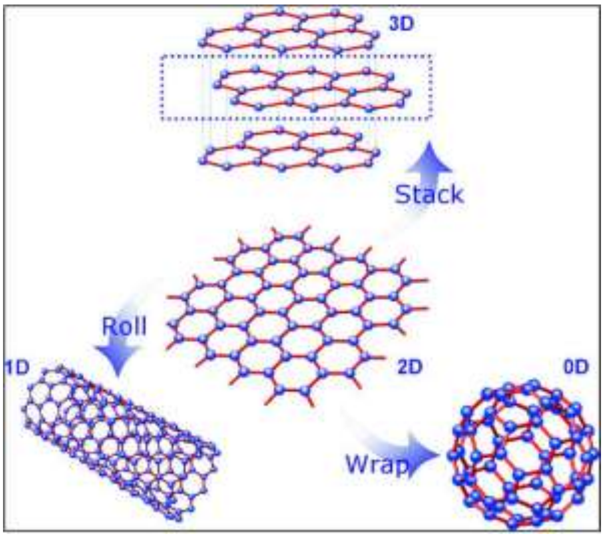

Figure 2-2: Graphene: The building blocks of carbon allotropes (Source:Garg et al. (2014))

Presently, carbon fibre is known to be one of the commonly used reinforcements in composites. It has microscale size characteristics and provides great strength and stiffness when used with polymers to form polymer matrix composites. Due to the impressive properties of carbon fibre, it is known that, for a specified volume fraction, as the diameter of the reinforcing fibres decrease, the interface between the reinforcement fibres and the matrix increases, resulting in a stronger multiphase and multiscale composite material (Boyer et al., 2012, Zhang et al., 2012).

Carbon nanofibres (CNF) are known to be similar to CNTs, but have distinct properties which affect the overall performance, as the size of the reinforcement fibres reduce to the nanoscale. CNTs became a more promising material to be used in composites due to its ability to provide high strength and stiffness to composites. As mentioned above, CNTs are cylindrical tubes which are formed by rolling nanosheets of graphene around a certain axis. In Figure 2-3, configurations of nanotubes are presented, where single-wall carbon nanotubes (SWCNT) are arranged by rolling a single nanosheet of graphene and multi-wall carbon nanotubes (MWCNT), being formed by more than one layer of graphene nanosheets.

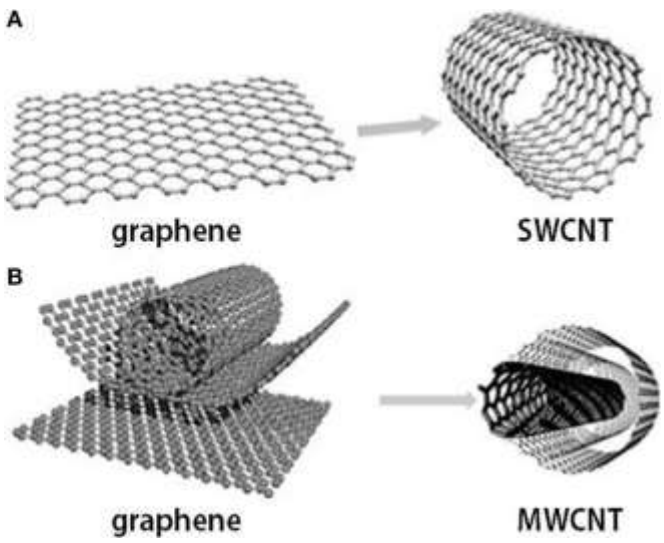

Figure 2-3 (A) Single-Wall CNT (SWCNT), (B) Multi-Wall CNT (MWCNT) (Source: Vidu et al. (2014))

The manufacturing of CNT nanocomposites is highly important in ensuring high quality material is obtained and it influences several factors in the CNT nanocomposite. In addition to hybridization, the dispersion and orientation of CNTs in the matrix is influenced by the manufacturing process. The properties of the composite materials are strongly affected by the interface between the matrix and the CNT reinforcement, where it is necessary to ensure a homogenous dispersion of CNTs is present within the matrix. Nonhomogeneous dispersion tends to result in crack initiation and possible failure of the material. The orientation of the CNT fibres affects the modulus and strength of the composite. Transversely isotropic composites are obtained by providing a uniform orientation of CNTs in the axial direction. This is to enable the modulus and strength to be higher in the axial direction compared to other directions of the element. Alternatively, isotropic composites are obtained by uniformly orientating the CNTs in all directions (x,y,z), which allows for equal moduli and strength in the composite (Bekyarova et al., 2007, Seidi and Kamarian, 2017, Qiu and Yang, 2017)

Chirality refers to the geometric property of a group of atoms in space or of a solid object, which results in it not being superimposable on its mirror image. The chiral vector C_h is composed of unit translational vectors a_1 and a_2, illustrated in Figure 2-4 and Figure 2-5, and is calculated as:

$$C_h = ma_1 + na_2 \tag{2-1}$$

where, m and n represents the number of hexagons covered by the unit vectors. The CNT axis is designated by vector T which is perpendicular to vector C_h (Kalamkarov et al., 2006). The chiral angle θ is defined as the angle between C_h and a_1 which changes from 0° to 30°, and is calculated as:

$$\theta = \sin^{-1}\left[\frac{\sqrt{3}m}{2\left(\sqrt{m^2+mn+n^2}\right)}\right] \tag{2-2}$$

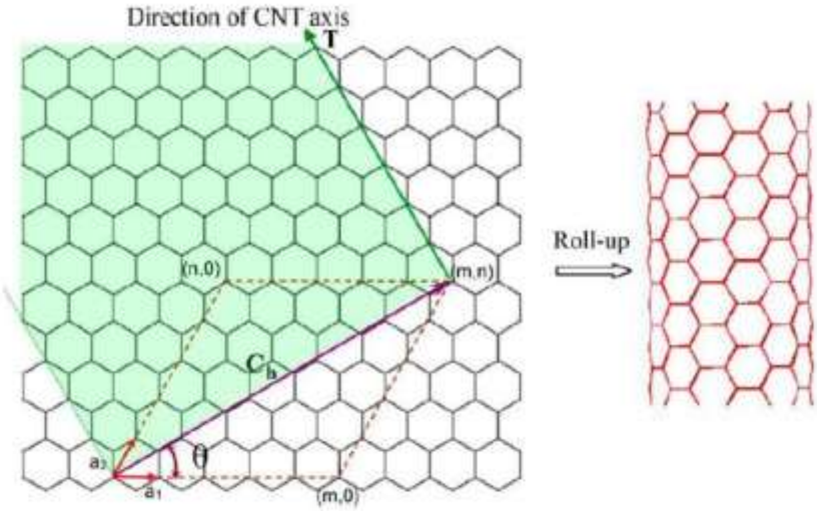

Figure 2-4: Roll-up vector defining the structure of carbon nanotubes (Source: Kalamkarov et al. (2006))

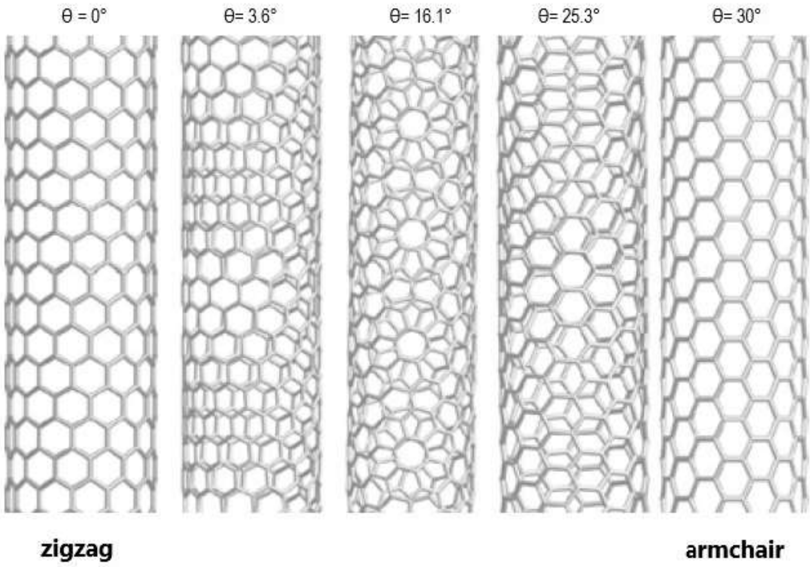

Figure 2-5: Structure of single-wall SWCNT with different chiral angles between 0° and 30° (Source: Sanchez et al. (2005))

According to Cao (2014), the Youngs Moduli and Poisson's ratio are not highly dependent on the chirality angles of the graphene sheets. Similarly, a study by Rajabpour et al. (2011) showed that this concept also applied to CNTs which resulted in a 0.25% difference in Youngs Modulus for chiral angles 0 to 30 degrees for carbon nanotubes.

By looking at a comparison between CNTs and other reinforcement materials, CNTs show to have extraordinary mechanical, thermal, and electrical properties. This can be seen by the high length to diameter ratio and the nature of the covalent bonds between the carbon atoms of the CNT. In Table 2-3, a comparison of the mechanical properties of CNT are shown with other materials used in engineering applications. CNTs have a much higher tensile strength than the other materials due to the covalent bonds and shows to be much stronger than steel. The incredible thermal and electrical conductivity shows why CNTs are so popular in the electronics industry.

Table 2-3: Representative properties of nanomaterials and other common materials in composites (after (Gong, 2018) and (Tserpes and Silvestre, 2014))

Materials	Tensile Strength	Thermal conductivity (W/mk)	Electrical conductivity (S/m)
Graphene	130 ± 10 GPa	(4,84±0.44) to $(5.3±0.48)x10^3$	7200
CNT	60 to150 GPa	3500 to 6000	3000 to 4000
Steel (Nanosized)	1.8 GPa	5 to 6	1 350 000
Kevlar fiber	3.6 to 4.1 GPa	0.04	Insulator

2.5 Fibre Reinforced Composites (FRC)

2.5.1 The Development of Composite Materials

The history of composite materials originated from as early as 1500 B.C. where strong and durable structures were developed by Egyptians and Mesopotamian settlers, utilizing mud and straw mixtures (Nagavally, 2017). Modern day engineered structures and building materials have greatly progressed from the common building materials like wood, stone, and mortar, owing to science and technological sophistication, which helped form advanced engineered materials. Composite materials are formed by using various other materials, with different properties and characteristics, which result in an enhanced material with improved properties as compared to its original constituents (Harris, 1991).

2.5.2 Constituents of FRCs

Fibre reinforced composites have been implemented in a wide range of engineering applications, from carbon fibre and fibreglass panels for vehicles and aircrafts, to retrofitting RC beams and structures using epoxy and fibre reinforcing. According to Cantwell and Morton (1991), carbon, glass and Kevlar fibres, which have been researched and examined extensively, have shown to possess high strength, stiffness, corrosion resistance, and improved fatigue properties. This was assessed through several applications which they have been put in. The fibres in composite structures are crucial for resisting the bulk of the applied loads and structural behaviour. The matrix material in the composite has equal importance as the reinforcing fibres used. It is responsible for ensuring there is an even distribution of the fibres in the layers and helps protect, align, and stabilize fibres to ensure that there is uniform stress transfer between the fibres in the composite. As with any type of composite, be it reinforced concrete elements or carbon fibre laminates, the bonding between the matrix materials and the fibre reinforcement is the an important factor in determining the overall mechanical and physical performance of the material (Prashanth et al., 2017).

Past studies have incorporated natural fibres in composites to adopt a green approach for new engineering materials. Velmurugan and Manikandan (2005) developed a glass fibre and palmyra natural fibre hybrid composite. The authors investigated the use of natural fibres as reinforcement with polymer materials, with results highlighting and showing the significant importance of being eco-friendly and contributing to sustainable solutions. The overall properties of the hybrid composite material were greatly improved by introducing high strength synthetic glass fibres to the palmyra fibre hybrid material.

Other beneficial studies include the retrofitting and rehabilitation of structures. Dasgupta Dasgupta (2018) conducted a study which investigated the numerous applications of fibre reinforced polymers (FRP) in the repairing and retrofitting of concrete beams and structures. The purpose of retrofitting structures was to allow for an increased design life of the structure and to improve the durability of the structure against factors such as fatigue, corrosion, and seismic responses.

2.5.3 Classification of Composite Materials

Composite materials or composite structures are classified depending on the properties of the constituents of the material. This refers to the fibre reinforcement, the matrix material, and the interface between the two (Yang et al., 2012). Figure 2-6 shows the classification of composite materials determined from the reinforcement material and the matrix material used. According to Park and Seo (2011), there need to be various chemical and mechanical tests conducted on each element in order to obtain the overall properties of the composite material, and to determine the suitable application for it.

Taking graphene as an example; defects and grain boundaries with samples on a macroscopic level is dependent on the environment it is exposed to and the production process used. According to Li et al. (2008), some of the most commonly used techniques for preparing graphene include: exfoliation or separation, chemical vapour deposition (CVD) and the reduction of graphene oxide. Each of these methods can successfully produce graphene, but the quality and properties of the product obtained depending on each process (Kim et al., 2010).

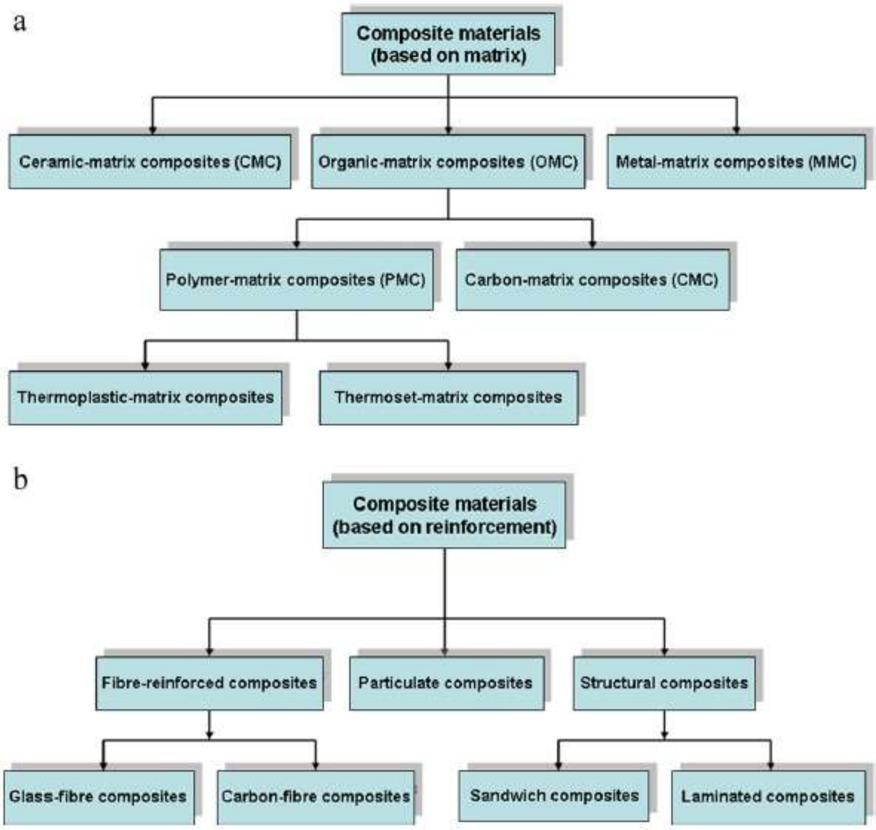

Figure 2-6: Composite materials: (a) Based on matrix material; (b) Based on reinforcement material (Source: Yang et al. (2012))

As mentioned in section 2.4, the dispersion and orientation of the reinforcement fibres plays a huge role in determining the type of composite and the elastic properties that the composite tend to present. A study by Madeo (2015) investigated types of fibrous composite reinforcements. This study provided conclusive evidence that woven fibre reinforcements can be classified as materials with orthotropic elastic properties. This is due to the fibres being woven in two directions irrespective of the weave pattern or different types of fibres used.

2.6 Micro-scale Modelling

Studies of elastic stress and displacement fields around dislocations, by Volterra (1907), initiated the theories and concepts of micromechanics. In recent years, with the increase of research and development in the material science industry, much attention has been given to the micromechanical modelling of solids. This is due to the fact that most materials have heterogeneous microstructures which influences the deformational behaviour of the macrostructure of the material (Sadd, 2014). For this, computational micromechanics have proven to yield a suitable framework in order to obtain detail predictions of local deformation mechanisms in heterogeneous materials, which result in the effective elastic properties of the composite material.

Numerical investigations and structural analysis of composites are essential in order to evaluate the performance and parameters of the structure and the material used with it. This is made possible by numerical equations and relationships which help model the materials and the structure holistically. These are categorised under hierarchical multi-scale modelling (HMM), where nano and micro scale elements are performed with semi-continuum modelling, and meso and macro scale elements falling within micromechanical models (Rafiee and Eskandariyun, 2019). Contained in Table 2-4 is the modelling methods and the involved parameters for multiscale modelling of CNT reinforced composites, with a representative volume element (RVE) defined for each scale.

Table 2-4: Effective scales of involved parameters and modelling methods at each scale (after Rafiee and Eskandariyun (2019))

Effective scale	Involved parameters	Modelling method
Nano	Molecular interactions of carbon-carbon bonds	Semi-continuum modelling through FEM
Micro	Interactions between CNTs and surrounding polymer	
Meso	Dimensions and orientations of CNTs	Micromechanical rules
Macro	Agglomeration and inhomogeneous dispersion of CNTs	Generalised methods of cell (GMC)

Sadd (2014) addressed micromechanical models based on linear elastic responses. For the dislocation modelling method, internal microstructural defects/imperfections were considered based on the atomic lattice structure of the material. This applies to edge and screw dislocations, which are two of the most common types of imperfections. For modelling which does not include imperfections like the edge and screw dislocations, elastic models are developed using singular stress states. This includes a variety of force and moment systems, which yields stress, strain, and displacement fields. Other models include materials with distribute cracks, materials with voids, micropolar and couple stress theory, and doublet mechanics.

Micromechanical modelling is an essential tool for analysing failure in advanced composite materials. Mccarthy and Vaughan (2015) investigated failure criteria using micromechanical models for the generation of failure surfaces from mechanical and thermo-mechanical loadings, and the bonding of composite joints. Material properties were easily modelled using micromechanics which enabled an interactive failure criterion. According to the authors, thermal residual stresses have a positive effect on the failure strength when subjected to tension-dominated loading and a slightly negative effect when subjected to shear dominated and compression-dominated loading. For bonded composite joints, failure occurs mainly at the bond lines due to adhesive properties, and weak points which were formed from the debonding of the fibres.

The fabrication technique and the quality of the constituent materials (fibre, CNT, matrix) greatly affects the abilities of the materials to bond with each other and the overall performance of the composite. According to Rafiee et al. (2018), there are two known procedures for manufacturing multiscale CNT/polymer nanocomposites. The first method is illustrated in Figure 2-7, by dispersing CNTs in the polymer matrix, and thereafter infusing the fibre reinforcement within the CNT/polymer nanocomposite. The second method adopts a slightly different approach, where the CNTs are infused with the fibres and then infused with the matrix.

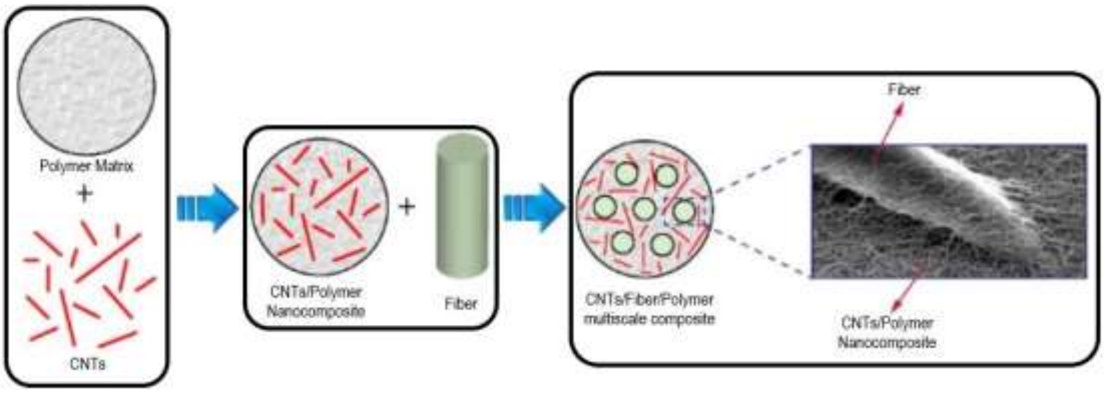

Figure 2-7: Dispersion of CNTs in polymer matrix, thereafter fibres in CNT/polymer nanocomposite (Source: Rafiee et al. (2018))

In this study, the effective material properties of the multiscale CNT/polymer nanocomposite were obtained using the procedure in Figure 2-7. Halpin-Tsai equations were used for the CNT/polymer nanocomposite. and fibre micromechanics for the latter. The summary of equations used for the modelling of the 3-phase multiscale CNT/polymer nanocomposite are briefly explained in the sections 2.6.1 and 2.6.2

2.6.1 Two-phase CNT reinforced matrix Halpin-Tsai equation formulation

The Halpin-Tsai equations for the Youngs modulus of the CNT reinforced matrix were calculated from Rafiee et al. (2018). where subscripts CNT/M and M denote the properties of the CNT reinforced matrix and unreinforced matrix respectively.

$$E_{CNT/M} = \frac{E_M}{8}\left[5\left(\frac{1+2\beta_{dd}V_{CNT}}{1-\beta_{dd}V_{CNT}}\right)+3\left(\frac{1+2\left(l_{CNT}/d_{CNT}\right)\beta_{dl}V_{CNT}}{1-\beta_{dl}V_{CNT}}\right)\right] \tag{2-3}$$

$$\beta_{dd} = \frac{\left(E_{CNT}/E_M\right)-\left(d_{CNT}/4t_{CNT}\right)}{\left(E_{CNT}/E_M\right)+\left(d_{CNT}/2t_{CNT}\right)} \tag{2-4}$$

$$\beta_{dl} = \frac{\left(E_{CNT}/E_M\right)-\left(d_{CNT}/4t_{CNT}\right)}{\left(E_{CNT}/E_M\right)+\left(l_{CNT}/2t_{CNT}\right)} \tag{2-5}$$

In the preceding equations, l_{CNT} , d_{CNT}, t_{CNT} notates the length, diameter, and thickness of the carbon nanotubes respectively. The Poisson's ratio and the shear modulus of the 2-phase CNT reinforced matrix is given by:

$$v_{CNT/M} = v_{CNT}V_{CNT} + v_M\left(1-V_{CNT}\right) \tag{2-6}$$

$$G_{CNT/M} = \frac{E_{CNT/M}}{2\left(1+v_{CNT/M}\right)} \tag{2-7}$$

The volume content of carbon nanotubes V_{CNT} is given by the equation (2-8) with respect to the weight fraction of the carbon nanotubes by manipulation of mass and density units.

$$V_{CNT} = \frac{W_{CNT}}{W_{CNT}+\left(\rho_{CNT}/\rho_M\right)\left(1-W_{CNT}\right)} \tag{2-8}$$

The density of the carbon nanotube reinforced matrix can be calculated using (2-8) and the elastic properties of the matrix.

$$\rho_{CNT/M} = \rho_{CNT}V_{CNT} + \rho_M\left(1-V_{CNT}\right) \tag{2-9}$$

2.6.2 Three-phase fibre/CNT reinforced matrix composite

The elastic moduli and density of the three-phase laminate are defined using the fibre micromechanical equations for the overall composite model. (Rafiee et al., 2018, Gholami et al., 2018)

$$E_{11} = E_{F11}V_F + E_{CNT/M}\left(1 - V_F\right) \tag{2-10}$$

$$E_{22} = \left(\begin{array}{l} \dfrac{V_F}{E_{F22}} + \dfrac{1-V_F}{E_{CNT/M}} \\ -V_F\left(1-V_F\right)\dfrac{v_F^2\, E_{CNT/M}/E_{F22} + v_{CNT/M}^2\, E_{F22}/E_{CNT/M} - 2v_F v_{CNT/M}}{V_F E_{F22} + \left(1-V_F\right)E_{CNT/M}} \end{array} \right)^{-1} \tag{2-11}$$

$$G_{12} = \left(\frac{V_F}{G_F} + \frac{1-V}{G_{CNT/M}} \right)^{-1} \tag{2-12}$$

$$v_{12} = v_{F12}V_F + v_{CNT/M}\left(1 - V_F\right) \tag{2-13}$$

The overall density for the 3-phase multiscale CNT/fibre/polymer nanocomposite is given by

$$\rho = \rho_F V_F + \rho_{CNT}V_{CNT} + \left(1 - V_F - V_{CNT}\right)\rho_M \tag{2-14}$$

2.7 Vibration of Composite Structures

Structural vibration is a phenomenon that occurs very frequently on structures, depending on the environment they're situated in. For example, buildings and skyscrapers are prone to vibrations caused by seismic, wind and other induced loads, whilst other structures like motor vehicle and aircrafts panels are subject to aerodynamic dynamic forces, and vibrations due to mechanical components. External forces, such as those mentioned above, prompt the structure to vibrate at its natural frequency. In simple terms, the nature of the vibration, or frequency, is influenced by the mass and stiffness of the system. For any structure to be within safe limits, the natural frequency of the structure would need to be relatively higher than the operating frequency when loads are being applied to it. Such considerations are made when designing structures and the materials they comprise of. The types of materials used play a crucial role in providing strength and stiffness in order to withstand and minimise the effects from external forces and vibrations.

In several studies, CNTs have been investigated in composite structures under free and forced vibration responses and buckling resistance. The use of multiphase and multiscale composites has provided improved stiffness and flexural behaviour which resulted in higher natural frequencies and buckling loads. This was due to the improved mechanical and physical properties from the synergistic effects of the constituents, and the combination of other physical characteristics in the composite (Díez-Pascual et al., 2014).

Ebrahimi and Dabbagh (2019) conducted an analytical investigation on the vibration response on multi-scale hybrid nanocomposite plates based on a Halpin-Tsai homogenization model. Results showed that the natural frequency of the composite was amplified by adding either fibre material by volume fraction or increasing CNT by weight fraction.

Ahmadi et al. (2018) conducted a free and forced vibrational analysis on a 3-phase, carbon fibre (CF)/CNT/reinforced polymer hybrid composite. Due to the covalent sp^2 bonds between the carbon atoms in the CNTs, it resulted in an exceptionally high tensile strength and Youngs Modulus which makes the CNTs one of the strongest and stiffest materials available. These properties significantly improved the vibration behaviour of the CF/CNT/polymer hybrid composite.

Bekyarova et al. (2007) noted a 30% improvement of the interlaminar shear strength with a 3-phase CNT/CF/epoxy laminate compared to a 2-phase CF/epoxy laminate. Other similar investigations where conducted in Ahmadi et al. (2017), Ebrahimi and Habibi (2018), Inam et al. (2010), Jamal-Omidi and Shayanmehr (2018), where CF/CNT reinforced laminates were modelled under vibration, and buckling, which showed the significant improvement of frequencies and buckling loads in multiphase, and multiscale composites

According to Reddy (2003), the analysis of composite plates are formed on these approaches:

- Equivalent single-layer plate theories (2D)
- Three dimensional elastic theories (3D)
- Multiple model methods (2D and 3D)

The Equivalent single-layer plate theories (ESL) consist of the classical laminated plate theory and shear deformation plate laminate theories. The ESL theories are derived from 3D elastic theories using assumptions for the kinematics of deformations which allows a reduction of a 3d problem to a 2d problem. For the three-dimensional elastic theories, traditional 3D elasticity formulations and layer wise theories are implemented, where each layer or ply is modelled as an individual 3-dimensional element.

2.8 Optimization of Composite Structures

2.8.1 Optimization Algorithms

Optimization is a tool which is used in almost every engineering and production process in order to produce the best result. This can be achieved by trying to minimize factors such as materials, cost, and energy, which result in a maximised profit, performance, or output. For any optimization problem to function successfully, there needs to be a suitable optimization algorithm which uses an efficient numerical simulator and all of which supports the physical processes of the model and its constraints. The basic process for any optimization is shown in Figure 2-8.

According to Yang (2013), the three main issues in optimization are, the efficiency of the algorithm, the efficiency and accuracy of the numerical solver, and the allocation of the suitable algorithm. Despite considering all these issues, it is still difficult in choosing the correct algorithm since the efficiency of the algorithm depends on several factors within the algorithm and the optimization problem. Some of optimization algorithms used in composite and structural applications are mentioned in this section.

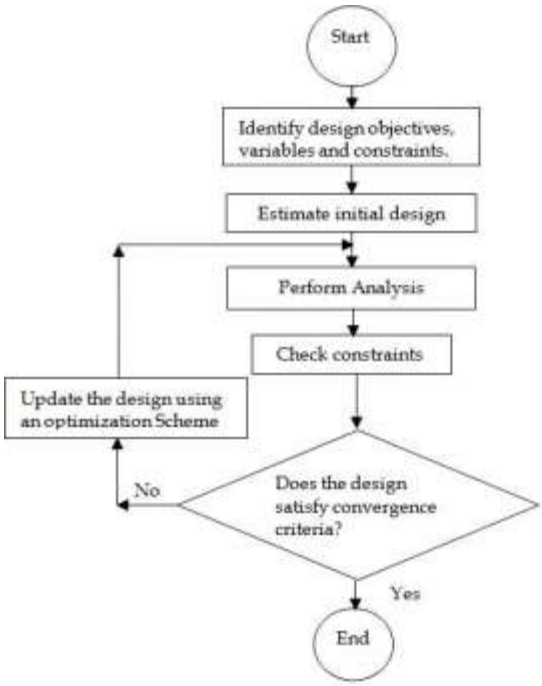

Figure 2-8: Design optimization process (Source: Maalawi (2018))

The Genetic Algorithm (GA) is one of the frequently used algorithms in composite optimization. It is a search and optimization algorithm which is based on Darwin's evolution of biological systems, observed in nature. For each iteration, it determines a solution from the previous iteration, directing the optimal solution to converge after a certain number of iterations. The algorithm considers the initial parameters as parents, and thereafter calculates new parameters based on the initial ones, moving down generations until the entire population or many generations reaches an optimal solution. Like the GA, the Simulated Annealing (SA) optimization algorithm is one of the metaheuristic methods. It is based on the simulation of thermal annealing of heated bodies. It conducts a random search using a Markov chain and accepts changes which improve the objective function and converges to an optimal solution when the prescribed tolerance is reached (Yang, 2013). The Particle Swarm Optimization (PSO) algorithm is similar to the GA, where it is formulated based on behaviour which occurs in nature such as fish schooling and insect swarms. The algorithm searches within the objective function by changing the trajectory of each particle, allowing it to follow the present optimal particle in each iteration.

For non-linear programming and constrained optimization, Sequential Quadratic Programming (SQP) is known to be the best technique in terms of accuracy and efficiency (Morshed and Asgharpour, 2014). Figure 2-9 outlines the flow of processes for the SQP method, where the calculation of the Hessian matrix and the quadratic sub-problems fall as the core structure in the whole process. Aktemur and Gusseinov (2017) investigated using different optimization algorithms to solve Golinski's speed reducer problem. In Table 2-5, the GA and SA arrived at the optimal solution while, the SQP method solves the problem much faster. According to the authors, there are some pros and cons to using SQP since it is a local optimizer while the other methods being global optimizers.

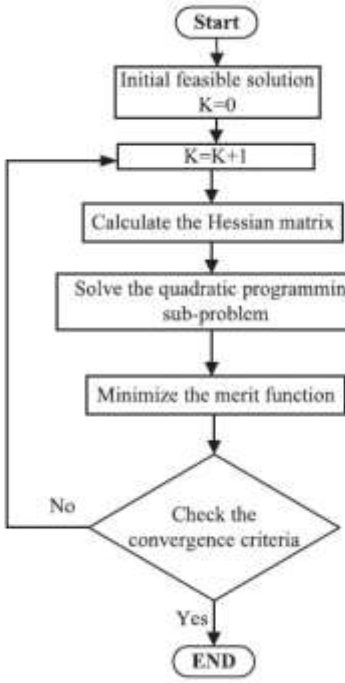

Figure 2-9: The flowchart of the SQP technique (Source: (Morshed and Asgharpour, 2014))

Table 2-5:Comparison of SQP, GA, SA and PSO optimization algorithms (after Aktemur and Gusseinov (2017)

Solution	SQP	GA	SA	PSO	GA+fmincon
Objective Value	2994.36	2703.59	2730.74	2905.68	2994.36
Function Evaluation	80	45499	17339	7910	43299
Computation Time	0.642	7.347	17.119	1.094	6.971
Ease of Implementation	Difficult	Medium	Medium	Medium	Easy

2.8.2 Optimal Composite Design

This current study investigates the lightweight design of advanced composites. This is an innovative approach containing multiscale, micro and nano, reinforcement material such as fibres and CNTs. The main objective is to minimize the weight of the composite whilst still being able to achieve high frequency resistances which is subject to a frequency constraint. This is achieved by optimizing the design variables such as stacking sequence, ply angles, thickness of plies and amount of reinforcement material in the composite. Nikbakt et al. (2018) stated that the type of optimization problem is based on the quality and quantity of the design variables and the objective functions. In composite lamina design, the lamina thickness and the angle are the common design variables used. Such considerations are based on the manufacturing precision and the feasibility of the optimal solution still being achieved after rounding off values to the nearest discrete manufacturable value (Akbulut and Sonmez, 2011). Mentioned below are a number of sources that used optimization for composite laminate design, using different techniques, variables, and analysis methods.

The Genetic Algorithm (GA) was the optimization method used in several studies and has been one of the commonly used methods for the optimal design of composites. In a study by Lopez et al. (2009), a minimum weight and minimum material cost optimization was solved by a GA. The ply orientations, number of layers and the material in the layers were assigned as design variables. Cardozo et al. (2011) investigated three optimization problems using a GA, together with the Finite Element method (FEM) and Artificial Neural Networks (ANN), for a composite laminate plate. Results were obtained by comparing the two methods used with the GA. The two methods produced similar results when used with the GA however, the computational time for the GA-ANN was better than the GA-FEM.

Assie et al. (2012), carried out an investigation for weight optimization using the GA and the Tsai-Wu failure criterion. This was achieved by optimizing the orientation angle and the thickness of the laminates in the composite plate. Pelletier and Vel (2006) presented a multi-objective optimization study by employing a non-dominated sorting genetic algorithm (NSGA-II) for laminate composite design. Liu et al. (2015) used the permutation genetic algorithm (permGA) by specifying the material volume as the objective function for an aircraft wing. The min weight design of the aircraft wing was achieved by a bi-level optimization strategy. The top-level optimization was solved using the first order optimization method available in ANSYS. For the bottom level optimization, the stacking sequence was optimized from the calculated lamination parameters in the top-level optimization. The permGA was efficient for the bottom level optimization since no finite element simulation was needed.

Almeida and Awruch (2009) used FEM and GA for two multi-objective optimization problems for the design of lightweight laminate structures. One problem involved the weight and the cost being the objective functions, and the other involving the weight and the deflection as the objective functions. The performance of the optimization algorithm was assessed by means of reliability and computational cost.

The genetic algorithm (GA) and simulated annealing (SA) optimization techniques were used by Karakaya and Soykasap (2011). The optimization was successfully achieved for each method however, results showed that the GA is better suited for optimization with many design variables and runs faster with more successful function evaluations obtained. Optimal laminate design was also accomplished in other studies using the feasible direction method (FDM) by Lin and Yu (1991), and adaptive elitist differential evolution (aeDE) algorithm in (Vo-Duy et al., 2017).

Giambanco et al. (1999) performed an optimal design of a laminate plate. The objective was to minimise the weight by optimizing the distribution of the thickness of the plies in the laminate. This was done by making the thickness of the plies as the design variable. From a more recent study, it was noted by Liu and Paavola (2016) that having the fibre volume fraction as a design variable had a significant effect on the weight of the laminate. (Park et al., 2003) carried out a multiple-constraint optimization study to minimise the weight of the composite laminate.

In most cases, the geometry has an effect on the overall performance of the composite with optimal angles and optimal reinforcement materials. Adali and Verijenko (2001) investigated the optimum stacking sequence for hybrid laminates undergoing free vibration. Results showed that optimum material utilization was obtained by placing stronger material, with more reinforcement, in the surface layers and weaker material in the core layers. Another interesting result showed that the aspect ratio influences the optimal stacking sequence. For aspect ratios between 0.2 and 0.6 the optimal stacking sequence was 0°, for aspect ratios between 0.7 and 1.4 was ±45°, and 1.5 to 2 was 90°.

A layer-wise optimization approach (LOA) was presented by Hansel and Becker (1999), using a heuristic optimization algorithm. A similar layer-wise optimization approach was carried out by Narita (2003). This was to optimize the fibre angles for the maximum fundamental frequency which was determined sequentially from the outermost layer to the innermost layer. A more recent study by An et al. (2019) solved the optimization of the laminate stacking sequence, which was by maximising the natural frequency and buckling load of a laminate cylinder and laminate plate. Wu and Viquerat (2017) optimized the natural frequency with respect to the fibre orientation angles and stacking sequences.

In structural design and analysis of structures, there are several tests conducted on a structure to reach a final solution or to conclude with the appropriate application of the structure and the materials. In this study, only the vibration analysis was investigated for the composite design. Other analysis such as bending and buckling using optimization are highlighted in (Ehsani and Rezaeepazhand, 2016, Shin et al., 1991, Adali et al., 1995, Aymerich and Serra, 2008, Ho-Huu et al., 2016).

2.9 Finite Element Analysis (FEA)

Finite element analysis and the finite element method (FEM) are methods used for the verification of the vibration analysis method in this present study. The finite element method is a numerical method used for solving mathematical and engineering problems. It has been used in typical engineering applications such as structural analysis, fluid dynamics, heat transfer, and electromagnetic potential (Logan, 2007). The solutions for the FEM formulated using a system of algebraic equations, which differ from analytical solutions that use partial differential equations. FEA uses a process known as discretization, where the body or solid is divided into smaller equivalent bodies, or finite elements, those of which are interconnected to each other at common points known as nodes. The solutions are obtained by determining the unknowns at each node which can be in the form of displacements, stresses or even temperatures, depending on the type of problem being solved. The finite element solution is then developed using the summation of the finite element analysis of each body or element (Logan, 2007). The performance and accuracy of the finite element solution is highly dependent on the discretization process. The higher number of finite elements used, provides higher accuracy for the solution for the specified problem.

According to (Logan, 2007), element stiffness matrices and element equations forms a background to any structure analysis problem. The element equations can be written in compact matrix form as shown in equation (2-15), and the global equations shown in equation (2-16).

Element equation matrix:

$$\{f\} = [k]\{d\} \tag{2-15}$$

where $\{f\}$ is the element nodal force vector, $[k]$ is indicated as the element stiffness matrix, and $\{d\}$ being the element displacement vector for unknown nodal degrees of freedom.

Global equation matrix:

$$\{F\} = [K]\{d\} \tag{2-16}$$

Where $\{F\}$ is the global nodal force vector, $[K]$ is the global stiffness matrix, and $\{d\}$ is the structure displacement vector of known or unknown nodal degrees of freedom.

2.10 Summary

Nanotechnology is a way of the future as innovative methods of implementing it are formed. In Africa, nanotechnology has a great potential in addressing some of the greatest challenges and help achieve sustainability goals. Nanomaterials like graphene and CNTs have immense potential in engineering applications, especially in structural engineering of composites for aircraft and aerospace. They have an incredible enhancement of strength and weight reduction properties in composites, especially with multiphase and multi scale materials.

Several publications have investigated the use of nanomaterials used in composite plates and being tested for vibration, buckling, and bending analysis. Micromechanics and Halpin-Tsai equations are used for modelling multiscale materials which help get the effective elastic properties of the composite material. Micromechanics are beneficial and there are multiple methods which can be used for different materials and to predict material failures.

Structural analysis can be done using numerical methods or analytically. The finite element method shows to be a very successful method for the analysis of structures, by means of numerical methods and finite element analysis. For analytical methods, the Ritz method is highly suitable for modelling laminate composite plates with simply supported boundary conditions using the classical laminate plate theory

Optimization algorithms have been very useful with providing the best design to reach the desired objective. Many optimization algorithms were assessed for the design of composite structures. From the list of algorithms, the genetic algorithm (GA) is the most efficient for composite laminate design, however for constrained optimization with linear programming, the sequential quadratic programming (SQP) method is known to be highly favourable.

CHAPTER 3 - METHODOLOGY

3.1 Introduction

In this chapter, the methodology of the optimal design of the composite plate is presented. The fundamental knowledge of composite engineering, vibration analysis and optimization techniques were required, and this was achieved through a literature study in chapter 2. The process highlighted in this chapter show the steps required for setting up the design problem. This begins with choosing the appropriate optimization algorithm. Next, micromechanics and modelling of the composite materials, followed by setting up the vibration analysis problem and the non-dimensional quantities. The last step is the core of this study, where all these concepts are integrated by the formulation of the optimization problems. The verification of the analytical method is presented, which provides confidence in the chosen methodology and the results that follow in the next chapter.

3.2 Sequential Quadratic Programming (SQP)

In the present work, the design objective, or objective function, is to minimise the weight of a simply supported (SSSS) laminate plate, subject to a frequency constraint. The optimization strategy involves the execution of a sequential quadratic programming algorithm (SQP), used in MATLAB, by means of introducing design variables and constraints for the optimization problem. The SQP is an iterative method which models the nonlinear programming problem, at a given approximate solution, by a quadratic programming subproblem. The solution to the quadratic subproblem is used to construct a better approximation for the next iteration by means of Newton and quasi-Newton methods for constrained optimization problems (Boggs and Tolle, 1995). From Bader (2009), the nonlinear problem involved in the optimization is shown as:

$$\begin{aligned} &\min \ f(x) \\ &\text{subject to}: \\ &\quad c_i(x) = 0 \quad i \in \varepsilon \\ &\quad c_i(x) \geq 0 \quad i \in I \end{aligned} \tag{3-1}$$

The inequality and equality constraints are linearized to obtain:

$$\begin{aligned} &\min_{p} f_k + \nabla f_k^T p + \frac{1}{2} p^T \nabla_{xx}^2 L_k p \\ &\text{subject to}: \\ &\quad \nabla c_i\left(x_k\right)^T p + c_i\left(x_k\right) = 0, i \in \varepsilon \\ &\quad \nabla c_i\left(x_k\right)^T p + c_i\left(x_k\right) \geq 0, i \in I \end{aligned} \tag{3-2}$$

3.3 Composite Modelling

This study entails the design of a 3-phase multiscale CNT/fibre/polymer nanocomposite. The crucial step starts with the modelling of the composite, by calculating the effective material properties from the CNTs, fibre and matrix elastic properties. The procedure is adopted from Rafiee et al. (2018), where the homogenization of the composite is conducted in two levels. First, a 2-phase CNT polymer matrix is formed using Halpin-Tsai equations mentioned in section (2.6.1). The final elastic properties are then obtained using the fibre micro-mechanic equations from section (2.6.2) which form the 3-phase multiscale CNT/fibre/polymer nanocomposite.

3.4 Vibration of laminate composites

3.4 1 Formulation of the Analytical Approach

For the vibration of the composite plate, a simply supported rectangular plate was considered. In Figure 3-1, the rectangular plate with total thickness **h** comprising of **N** orthotropic layers is shown. For this problem, the positive z-axis extends downwards from the midplane of the laminate and the kth layer is located between points $\mathbf{z_k}$ and $\mathbf{z_{k+1}}$ along the thickness of the plate (see Figure 3-1 (right)).

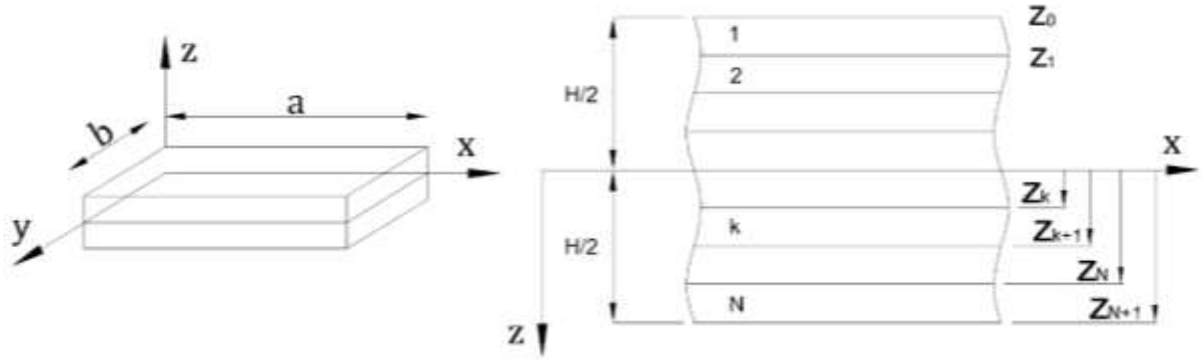

Figure 3-1: Coordinate system and layer numbering used for a laminate plate

Governing equations to laminate theories can be solved using analytical or numerical solutions. For this study, the analytical approach was adopted using the classical laminate plate theory (CLPT). From the numerous analytical methods out there, the Ritz method was employed for the composite plate which develops approximate solutions for the simply supported boundary conditions.

For the vibration analysis problem, the governing equation for natural vibration is given by (Reddy, 2003, p. 282):

$$D_{11}\frac{\partial^4 w_0}{\partial x^4}+2\left(D_{12}+2D_{66}\right)\frac{\partial^4 w_0}{\partial x^2\partial y^2}+D_{22}\frac{\partial^4 w_0}{\partial y^4}+I_0\ddot{w}_0-I_2\left(\frac{\partial^2\ddot{w}_0}{\partial x^2}+\frac{\partial^2\ddot{w}_0}{\partial y^2}\right)=0 \tag{3-3}$$

where,

$$\begin{aligned} I_0 &= \sum_{k=1}^{L} p_0^{(k)}\left(z_{k+1}-z_k\right) \\ I_2 &= \frac{1}{3}\sum_{k=1}^{L} p_0^{(k)}\left(z_{k+1}^3-z_k^3\right) \end{aligned} \tag{3-4}$$

The overall stiffness of the plate is denoted by:

$$D_{ij}=\frac{1}{3}\sum_{k=1}^{N}\bar{Q}_{ij}^{(k)}\left(z_{k+1}^3-z_k^3\right) \tag{3-5}$$

And the transformed stiffness terms, $\bar{Q}_{ij}$ can be expressed as:

$$\begin{aligned} \bar{Q}_{11} &= Q_{11}\cos^4\theta+2\left(Q_{12}+2Q_{66}\right)\sin^2\theta\cos^2\theta+Q_{22}\sin^4\theta \\ \bar{Q}_{12} &= \left(Q_{11}+Q_{22}-4Q_{66}\right)\sin^2\theta\cos^2\theta+Q_{12}\left(\sin^4\theta+\cos^4\theta\right) \\ \bar{Q}_{22} &= Q_{11}\sin^4\theta+2\left(Q_{12}+2Q_{66}\right)\sin^2\theta\cos^2\theta+Q_{22}\cos^4\theta \\ \bar{Q}_{66} &= \left(Q_{11}+Q_{22}-2Q_{12}-2Q_{66}\right)\sin^2\theta\cos^2\theta+Q_{66}\left(\sin^4\theta+\cos^4\theta\right) \end{aligned} \tag{3-6}$$

The plane stress-reduced stiffnesses for each layer is expressed as:

$$\begin{aligned} Q_{11} &= \frac{E_1}{1-v_{12}v_{21}}, \\ Q_{12} &= \frac{v_{12}E_2}{\Delta p}=\frac{v_{21}E_1}{\Delta p}, \\ Q_{22} &= \frac{E_{22}}{\Delta p}, \\ Q_{66} &= G_{12}, \\ \Delta p &= 1-v_{12}v_{21} \end{aligned} \tag{3-7}$$

The solution for the natural frequency (fundamental frequency) for the plate can be expressed as equation (3-8), where there is a unique frequency and mode shape for different values of m and n.

$$\omega_{mn}^2 = \frac{\pi^4}{\bar{I}_0 b^4}\left[D_{11}m^4\left(\frac{b}{a}\right)^4 + 2\left(D_{12}+2D_{66}\right)m^2n^2\left(\frac{b}{a}\right)^2 + D_{22}n^4\right] \tag{3-8}$$

where,

$$\bar{I}_0 = I_0 + I_2\left[\left(\frac{m\pi}{a}\right)^2 + \left(\frac{n\pi}{b}\right)^2\right] \tag{3-9}$$

The contribution of rotary inertia is very small but has an effect of reducing the natural frequency for any values of m and n. For this study, the rotary inertia was neglected ($I_2 = 0$), which makes it more comprehensive when obtaining the maximum natural frequency of the composite plate.

3.4.2 Formulation of the Non-Dimensional Solution

A benchmark must be set to assess the performance of the composite plate. For this, an unreinforced isotropic plate was used to evaluate the frequencies and weight when changing parameters of the composite plate.

The frequency of a reference unreinforced plate can be derived using the governing equations for free vibration of isotopic plates of uniform thickness. The exact vibration solution for rectangular plate with four edges simply supported is given from (Wang and Wang, 2013, p.141) using the exact vibration solution for thin isotropic plates.

$$\omega_{mn} = \sqrt{\frac{D}{\rho_M H}}\left[\left(\frac{m\pi}{a}\right)^2 + \left(\frac{n\pi}{b}\right)^2\right] \tag{3-10}$$

where D is the flexural rigidity denoted by the equation (3-11)

$$D = \frac{E_M H^3}{12\left(1-\nu_M^2\right)} \tag{3-11}$$

The utilization of these equations is discussed further in this chapter where the non-dimensional quantities are derived for the optimal design of the composite plate.

3.5 Formulation of the optimization problems

Five optimization problems are evaluated for the design of the composite laminate plate. The dimensions of the composite laminate are shown in Figure 3-2, where **a** and **b** are the dimensions in the **X-Y** direction. **H** represents the total laminate thickness in the **Z-**direction. The total number of layers in the composite is denoted as **N**. The design variables are fibre volume fraction (**V_F**), CNT weight fraction (**W_{CNT}**), fibre orientation angles (**θ**), and ply thickness ratio (**h/H**). These design variables are implemented but are limited by constraints set for each of them. The formulation of each optimization problem is briefly explained in the next sections.

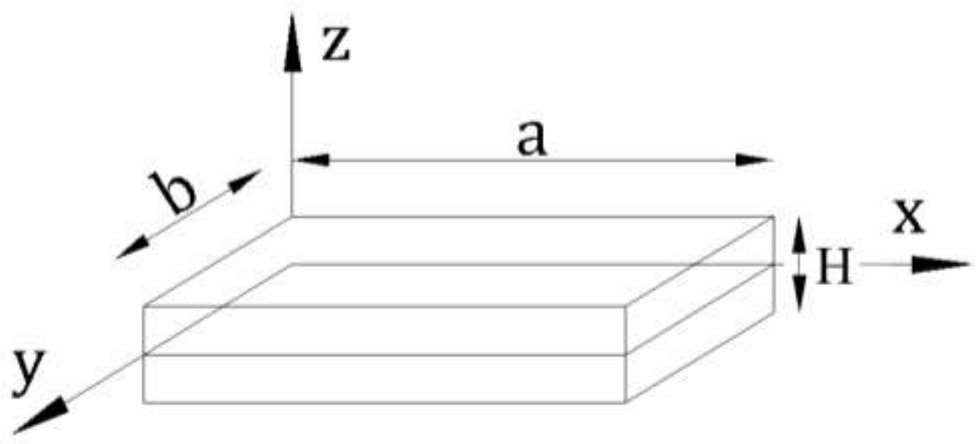

Figure 3-2: Geometry of the composite plate

3.5.1 Problem 1: 2-Phase Uniform Layer Thickness and Non-Uniform Distribution of Reinforcement Material (Design variable: V_F)

The first optimization problem involves the optimization of a 2-phase, fibre reinforced laminate, with uniform layer thickness along with non-uniform distribution of fibre in the layers. The volume of fibres in each layer is given by $Vol_{F\,i} = a\ b\ h\ V_{F\,i}$, where **h** is the layer thickness equivalent to H/N . The total volume of fibres in the N-layer laminate is given by $Vol_{F\ Total} = \sum_{i=1}^{N} Vol_{Fi} = a\ b\ h \sum_{i=1}^{N} V_{Fi}$. The maximum volume of non-uniformly distributed fibres in the laminate is given by $Vol_{F\max} = abHV_{F\max}$, where $V_{F\max}$ is the total volume fraction of fibres in the laminate. For the present study, the optimization for an 8-layered laminate with fibre volume fraction as a design variable is defined with the design constraints.

$$\min\ Weight:\ \mathrm{W}_L\ (V_F) = \sum_{i=1}^{8}(W_{Fi} + W_{Mi}) = abh\sum_{i=1}^{8}(\rho_F V_{Fi} + \rho_M(1-V_{Fi})) \tag{3-12}$$

$$\text{subject to}: \frac{\omega_{11}}{\omega_{\mathrm{mn}}} - \mathrm{f}_1 = 0 \tag{3-13}$$

$$\frac{1}{8}\sum_{\mathrm{i}=1}^{8} \mathrm{V_{Fi}} \leq \mathrm{V_{F\max}} \tag{3-14}$$

$$\mathrm{V_{FLower}} \leq \mathrm{V_{Fi}} \leq \mathrm{V_{FUpper}} \tag{3-15}$$

$$-90° \leq \text{fiber angle}\ \theta_{\mathrm{i}} \leq +90° \tag{3-16}$$

Equation (3-12) shows the objective function for the optimization problem. This is defined by the design variable $\mathbf{V_F}$ and the design constraints in equations (3-13) to (3-16). The frequency representing the plate under investigation $(\boldsymbol{\omega_{11}})$ is calculated as a function of $\mathbf{V_F}$ and $\boldsymbol{\theta}$, using equations (3-5) to (3-8). The frequency of the reference plate $(\boldsymbol{\omega_{mn}})$ is defined by equations (3-10) and (3-11) and the ratio $\frac{\boldsymbol{\omega_{11}}}{\boldsymbol{\omega_{mn}}}$, representing the non-dimensional frequency, should be equal to the frequency constraint limit $(\boldsymbol{f_1})$, shown in equation (3-13). The maximum fibre volume $V_{F\max}$ is constrained using equation (3-14). The limits for the fibre volume in each layer are defined, where the maximum fibre volume constraint for the overall laminate is still being satisfied. The upper and lower limits for the fibre angles are defined for every layer in the laminate. The optimal solution is assessed by analysing the parameters which contribute the minimum weight. This is by introducing a design efficiency factor η , which is the ratio of the weights of the fibre reinforced composite plate W_L, and the unreinforced reference plate W_0.

$$\eta = \frac{W_L(V_F)}{W_0(H_0(f_1))} = \frac{abh\sum_{i=1}^{8}(\rho_F V_{Fi} + \rho_M(1-V_{Fi}))}{abH_0\rho_M} \tag{3-17}$$

H_0 is derived considering the concept of the free vibration of isotropic plates by rearranging equation (3-10) in terms of the thickness **H**, and ω_{mn} calculated from equation (3-8).

$$H_0 = \frac{\omega_{mn}}{\sqrt{(E_M/(12\rho_M(1-v_M{}^2)))}\left((\frac{\pi m}{a})^2 + (\frac{\pi n}{b})^2\right)} \tag{3-18}$$

3.5.2 Problem 2: 3-Phase Uniform Layer Thickness and Non-Uniform Distribution of Reinforcement Material (Design variable: V_F)

This problem involves the optimization of a 3-phase, CNT/fibre reinforced laminate, with uniform layer thicknesses, uniform distribution of CNT and non-uniform distribution of fibre in the layers. The uniform distribution of CNT is assigned explicitly by the user whilst the distribution of fibre reinforcement in the layers are assigned optimally using the optimization algorithm. The optimization problem is defined as in problem 1 but with the addition of CNT as shown.

$$\begin{aligned} \min\ Weight:\ \mathrm{W}_L\ (V_F) &= \sum_{i=1}^{8}(W_{Fi} + W_{CNTi} + W_{Mi}) \\ &= abh\sum_{i=1}^{8}(\rho_F V_{Fi} + \rho_{CNT} V_{CNTi} + \rho_M(1 - V_{Fi} - V_{CNTi})) \end{aligned} \tag{3-19}$$

$$\text{subject to}: \frac{\omega_{11}}{\omega_{\mathrm{mn}}} - \mathrm{f}_1 = 0 \tag{3-20}$$

$$\frac{1}{8}\sum_{\mathrm{i}=1}^{8}\mathrm{V}_{\mathrm{Fi}} \le \mathrm{V}_{\mathrm{F\,max}} \tag{3-21}$$

$$\mathrm{V}_{\mathrm{FLower}} \le \mathrm{V}_{\mathrm{Fi}} \le \mathrm{V}_{\mathrm{FUpper}} \tag{3-22}$$

$$-90° \le \text{fiber angle}\ \theta_{\mathrm{i}} \le +90° \tag{3-23}$$

The design efficiency factor η , with the addition of CNT in the problem is defined as

$$\eta = \frac{W_L(V_F)}{W_0(H_0(f_1))} = \frac{abh\sum_{i=1}^{8}(\rho_F V_{Fi} + \rho_{CNT} V_{CNTi} + \rho_M(1 - V_{Fi} - V_{CNTi}))}{abH_0\rho_M} \tag{3-24}$$

3.5.3 Problem 3: 3-Phase Uniform Layer Thickness and Non-Uniform Distribution of Reinforcement Material (Design variables: V_F and W_{CNT})

In this optimization problem, a second design variable is introduced. This involves the optimization of the 3-phase, CNT/fibre reinforced laminate, with uniform layer thicknesses and non-uniform distribution of fibre and CNT in the layers. The optimization problem is defined as in problem 2 but with the distribution of fibre and CNT being optimized throughout the laminate. The minimum weight design is defined in the objective function, in terms of the two design variables. The constrains of the optimization problem is also defined.

$$\min \ Weight: \ W_L\,(V_F, W_{CNT}) = \sum_{i=1}^{8}(W_{Fi} + W_{CNTi} + W_{Mi}) = abh\sum_{i=1}^{8}(\rho_F V_{Fi} + \rho_{CNT} V_{CNTi} + \rho_M\,(1 - V_{Fi} - V_{CNTi})) \tag{3-25}$$

$$\text{subject to}: \frac{\omega_{11}}{\omega_{mn}} - f_1 = 0 \tag{3-26}$$

$$\frac{1}{8}\sum_{i=1}^{8} V_{Fi} \le V_{F\max} \tag{3-27}$$

$$V_{FLower} \le V_{Fi} \le V_{FUpper} \tag{3-28}$$

$$\frac{1}{8}\sum_{i=1}^{8} W_{CNTi} \le W_{CNT\max} \tag{3-29}$$

$$W_{CNTLower} \le W_{CNTi} \le W_{CNTUpper} \tag{3-30}$$

$$-90° \le \text{fiber angle}\ \theta_i \le +90° \tag{3-31}$$

The design efficiency factor η , with the addition of CNT in the optimization problem is defined as

$$\eta = \frac{W_L(V_F, W_{CNT})}{W_0(H_0(f_1))} = \frac{abh\sum_{i=1}^{8}(\rho_F V_{Fi} + \rho_{CNT} V_{CNTi} + \rho_M\,(1 - V_{Fi} - V_{CNTi}))}{abH_0\rho_M} \tag{3-32}$$

3.5.4 Problem 4: 3-Phase Uniform Layer Thickness and Non-Uniform Distribution of Reinforcement Material (Design variables: V_F, W_{CNT}, fibre angle)

For this optimization problem, the fibre stacking angle is introduced as the third design variable. The optimization problem is defined as in problem 3, with the distribution of fibre and CNT being optimized throughout the laminate and the optimal fibre angle of each layer to be obtained. The layer thickness is uniform whilst the distribution of reinforcement throughout the composite is non-uniform. The minimum weight objective function is defined with respect to the design variables for this optimization problem. The constraints and linear inequalities to the optimization problem is defined.

$$\min\ Weight:\ W_L\ (V_F, W_{CNT}, \theta) = \sum_{i=1}^{8}(W_{Fi} + W_{CNTi} + W_{Mi})$$
$$= abh\sum_{i=1}^{8}(\rho_F V_{Fi} + \rho_{CNT} V_{CNTi} + \rho_M (1 - V_{Fi} - V_{CNTi})) \tag{3-33}$$

$$\text{subject to}: \frac{\omega_{11}}{\omega_{\text{mn}}} - \text{f}_1 = 0 \tag{3-34}$$

$$\frac{1}{8}\sum_{\text{i}=1}^{8} \text{V}_{\text{Fi}} \le \text{V}_{\text{F max}} \tag{3-35}$$

$$\text{V}_{\text{FLower}} \le \text{V}_{\text{Fi}} \le \text{V}_{\text{FUpper}} \tag{3-36}$$

$$\frac{1}{8}\sum_{\text{i}=1}^{8} \text{W}_{\text{CNTi}} \le \text{W}_{\text{CNT max}} \tag{3-37}$$

$$\text{W}_{\text{CNTLower}} \le \text{W}_{\text{CNTi}} \le \text{W}_{\text{CNTUpper}} \tag{3-38}$$

$$-90° \le \text{fiber angle}\ \theta_{\text{i}} \le +90° \tag{3-39}$$

The design efficiency factor η , with the three design variables is defined as

$$\eta = \frac{W_L(V_F, W_{CNT}, \theta)}{W_0(H_0(f_1))} = \frac{abh\sum_{i=1}^{8}(\rho_F V_{Fi} + \rho_{CNT} V_{CNTi} + \rho_M (1 - V_{Fi} - V_{CNTi}))}{abH_0 \rho_M} \tag{3-40}$$

3.5.5 Problem 5: 3-Phase <u>Non-Uniform Layer Thickness</u> and Non-Uniform Distribution of Reinforcement Material (Design variables: V_F, W_{CNT}, fibre angle, thickness ratio)

This problem involves the optimization of a 3-phase laminate, with non-uniform layer thicknesses and non-uniform distribution of reinforcement in the laminate. The optimization problem is defined using four design variables, with the distribution of fibre and CNT being optimized throughout the laminate and the optimal fibre angle of each layer obtained. In the laminate, each layer thickness $\mathbf{h_i}$ is determined optimally using the optimization strategy. The volume of fibres in each layer is given by $Vol_{F\,i} = a\,b\,h_i V_{F\,i}$, where $\mathbf{h_i}$ is the layer thickness. The total volume of fibres in the N-layer laminate is given by $Vol_{F\,Total} = \sum_{i=1}^{N} Vol_{F\,i} = a\,b \sum_{i=1}^{N} h_i V_{F\,i}$. Similarly, the weight of CNT in each layer is given by $W_{CNT\,i} = a\,b\,h_i W_{CNT\,i}$, where $\mathbf{h_i}$ is the layer thickness and the total weight of CNT in the N-layer laminate is given by $W_{CNTTotal} = \sum_{i=1}^{N} W_{CNTi} = ab \sum_{i=1}^{N} h_i W_{CNTi}$. The optimization problem for an 8-layered laminate with V_F, W_{CNT}, fibre angle, and thickness ratio as design variables is defined with the design constraints.

$$\min\ Weight:\ W_L\,(V_F, W_{CNT}, \theta, \frac{h}{H}) = \sum_{i=1}^{8}(W_{Fi} + W_{CNTi} + W_{Mi}) \\ = ab\sum_{i=1}^{8}(\rho_F V_{Fi} h_i + \rho_{CNT} V_{CNTi} h_i + \rho_M h_i (1 - V_{Fi} - V_{CNTi})) \tag{3-41}$$

$$\text{subject to: } f_1(V_F, W_{CNT}, \theta, \frac{h}{H}) = f_1 \tag{3-42}$$

$$\frac{1}{H}\sum_{i=1}^{8} V_{Fi} h_i \le V_{F\max} \tag{3-43}$$

$$V_{FLower} \le V_{Fi} \le V_{FUpper} \tag{3-44}$$

$$\frac{1}{H}\sum_{i=1}^{8} W_{CNTi} h_i \le W_{CNT\max} \tag{3-45}$$

$$W_{CNTLower} \le W_{CNTi} \le W_{CNTUpper} \tag{3-46}$$

$$-90° \le \text{fiber angle } \theta_i \le +90° \tag{3-47}$$

$$\sum_{i=1}^{8} \frac{h_i}{H} = 1 \tag{3-48}$$

The design efficiency factor η, with the four design variables is defined as

$$\eta = \frac{W_L(V_F, W_{CNT}, \theta, \frac{h}{H})}{W_0(H_0(f_1))} = \frac{ab\sum_{i=1}^{8}(\rho_F V_{Fi} h_i + \rho_{CNT} V_{CNTi} h_i + \rho_M h_i (1 - V_{Fi} - V_{CNTi}))}{abH_0 \rho_M} \tag{3-49}$$

3.6. Verification

In this section, the verification of the methodology for the vibration analysis is presented. This is accomplished by comparing the results from published literature to the results using the analysis method in this present study. These results are further analysed with the numerical results obtained, using commercial software (ANSYS), using the design parameters E_1=60.7GPa, E_2=24.8GPa, G_{12}=12.0GPa and v_{12}=0.23 for E-glass/epoxy specified in a study by Wang et al. (2012). The authors investigated the free vibration behaviour on a 3-layered simply supported anisotropic rectangular plate using the discrete singular convolution (DSC) algorithm. The non-dimensional frequency was given by $\varpi = \omega \alpha^2 \sqrt{\rho h / D_0}$ and was used to rationalise the results from ANSYS and from the analysis method of this present study. The model of the simply supported composite plate using ANSYS is shown in Figure 3-3. The comparisons of the non-dimensional frequency from using alternate methods are shown in Table 3-1 and shows that results from the methods are within close range of each other.

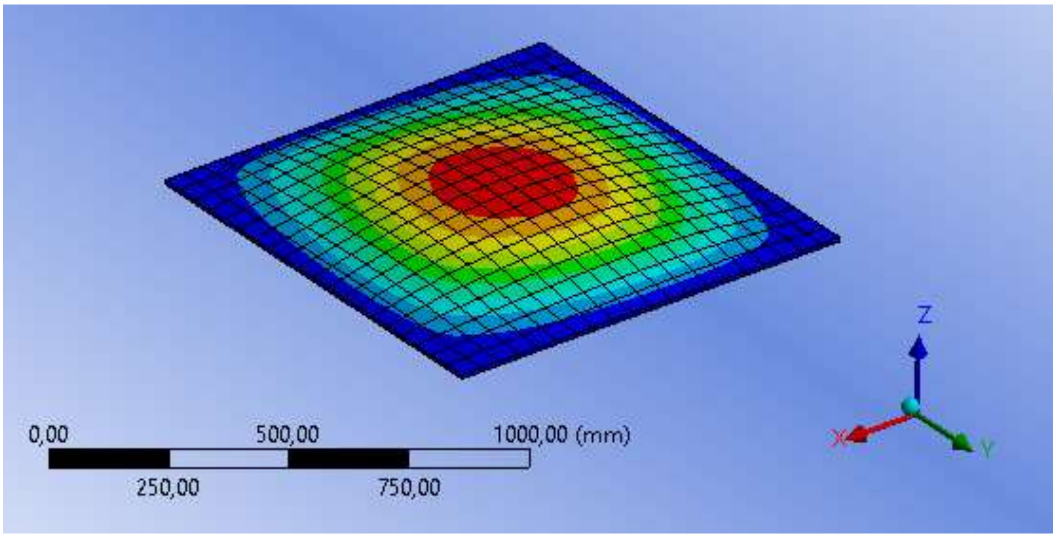

Figure 3-3: ANSYS model of the simply supported composite plate

Table 3-1: Comparison of numerical results for a 3-layered SSSS square laminate

Stacking sequence	Methods	Non-dimensional frequency (Mode 1)
[0°/0°/0°]	Present Method	15.115
	Commercial software	14.863
	DSC (Wang et al., 2012)	15.171
	Ritz method (Leissa and Narita, 1989)	15.190
[15°/-15°/15°]	Present Method	15.491
	Commercial software	15.294
	DSC (Wang et al., 2012)	15.369
	Ritz method (Leissa and Narita, 1989)	15.430
[30°/-30°/30°]	Present Method	16.215
	Commercial software	15.902
	DSC (Wang et al., 2012)	15.583
	Ritz method(Leissa and Narita, 1989)	15.90
[45°/-45°/45°]	Present Method	16.566
	Commercial software	16.249
	DSC (Wang et al., 2012)	16.082
	Ritz method (Leissa and Narita, 1989)	16.140

For this study, CNT and glass fibres are used for the reinforcement of the composite plate, which makes it a 3-phase laminate plate using materials with and multi scale properties. The material properties for the carbon nanotubes, glass fibre and epoxy matrix are listed in Table 3-2 similar to those by (Gholami et al., 2018, Rafiee et al., 2018, Rafiee and Eskandariyun, 2019). The following dimensions are used for the CNTs: $l_{CNT}=25\mu m$, $d_{CNT}=1.4nm$, $t_{CNT}=0.34nm$. The properties defined here are used in the Halpin-Tsai and fibre micromechanics equations to obtain the effective material elastic properties for the composite plate.

Table 3-2: Material properties

Material	*E* (GPa)	*G* (GPa)	ν	Density (kg/m^3)
Carbon Nanotubes	640	*E*/(2(1+í))	0.27	1350
Matrix	3.5	*E*/(2(1+í))	0.35	1200
Glass fibres	72.4	*E*/(2(1+í))	0.20	2400

The initial verification method involved verifying the vibration analysis method with results from published sources. Table 3-3 shows the verification of the present methodology using carbon nanotubes and glass fibres in the composite. The results using the commercial software (ANSYS) closely matches the results formulated with the methodology in the present study. This indicated that the accuracy of the solutions obtained are satisfactory and suitable for further analysis for the optimization problems hereafter.

Table 3-3: Comparison of Numerical results with commercial software for 3-ply CNT/Fibre reinforced laminate

Material Content	Stacking Sequence	Non-dimensional frequency (Mode 1)	
		Present Study	Commercial Software
V_f=30% W_{CNT}=1%	[0°/0°/0°]	13.760	13.172
	[15°/-15°/15°]	14.385	13.791
	[30°/-30°/30°]	15.559	14.727
	[45°/-45°/45°]	16.114	15.294
V_f=30% W_{CNT}=5%	[0°/0°/0°]	16.535	16.426
	[15°/-15°/15°]	16.860	16.782
	[30°/-30°/30°]	17.492	17.359
	[45°/-45°/45°]	17.800	17.678
V_f=60% W_{CNT}=1%	[0°/0°/0°]	13.411	13.250
	[15°/-15°/15°]	14.085	14.177
	[30°/-30°/30°]	15.346	15.423
	[45°/-45°/45°]	15.938	15.996

Furthermore, in order to verify an optimization problem, there would need to be a comparison to show what the likely solution would arrive to by using an alternative analysis method. In addition to the results in Table 3-3, simulations were conducted using an 8-layered laminate which is in context to this present study. Figure 3-4 presents the results using commercial software (ANSYS) for different amounts of reinforcement materials, resulting in a corresponding non-dimensional frequency and non-dimensional weight. The details to the verification using the 8-layered laminate is provided in Table 3-4. The trend in these results show that, as the non-dimensional frequency increases towards a given limit, the non-dimensional weight will decrease accordingly. This can be seen where the non-dimensional weight decreases towards 0.64 for a frequency reaching towards 1.69, hence reaching the similar optimal solution at the given limit when evaluated with using the methodology of this present study.

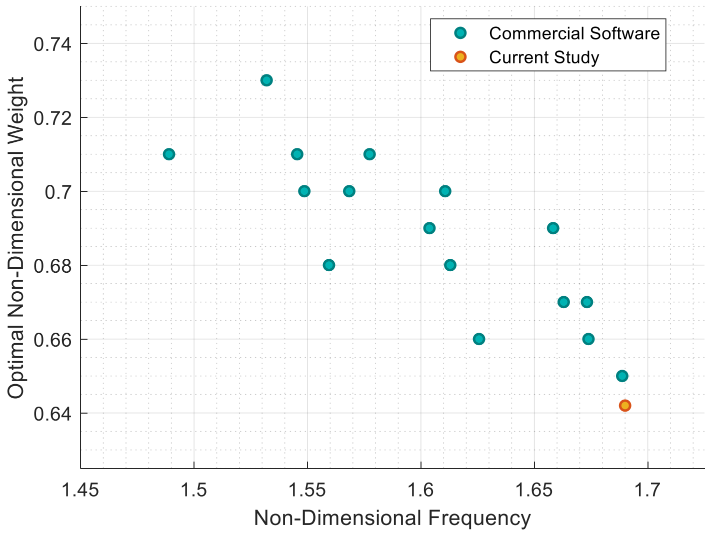

Figure 3-4: Verification of the weight optimization methodology

Table 3-4: Comparison of Numerical results with commercial software for 8-layer CNT/Fibre reinforced laminate

Numerical results using commercial software			
CNT Wt %	Fiber Vol %	Non-Dimensional Weight	Non-Dimensional Frequency
0.00125	[0.2/0/0/0]s	0.71	1.489
0.00125	[0.25/0/0/0.2]s	0.73	1.532
0.00125	[0.25/0/0/0.1]s	0.71	1.545
0.00125	[0.2/0.1/0/0]s	0.70	1.549
0.00125	[0.25/0/0/0]s	0.68	1.559
0.00125	[0.25/0/0.1/0]s	0.70	1.568
0.00125	[0.25/0/0.2/0]s	0.71	1.577
0.00125	[0.2/0.2/0/0]s	0.69	1.604
0.00125	[0.2/0.2/0.1/0]s	0.70	1.611
0.00125	[0.25/0.1/0/0]s	0.68	1.613
0.00125	[0.3/0/0/0]s	0.66	1.626
0.00125	[0.35/0/0/0.2]s	0.69	1.658
0.00125	[0.25/0.2/0/0]s	0.67	1.663
0.00125	[0.35/0/0/0.1]s	0.67	1.673
0.00125	[0.3/0.1/0/0]s	0.66	1.674
0.00125	[0.35/0/0/0]s	0.65	1.689
Optimal results using methodology for the present study			
CNT Wt %	Fiber Vol %	Non-Dimensional Weight	Non-Dimensional Frequency
0.00125	[0.3394/0/0/0]s	0.642	1.69

3.7 Summary

The sequential quadratic programming (SQP) algorithm has been chosen for the weight optimization of the composite plate. Fibre micromechanics and Halpin-Tsai equations are used to obtain effective material properties for the 3-phase CNT/fibre reinforced nanocomposite. Five optimization problems were defined in this chapter. The formulation of the vibration analysis method was presented using the Ritz method. The first 4 problems were defined using uniform thickness of the layers in the composite. The first problem specified the optimization of a 2-phase composite with fibre volume fraction as the design variable. The second problem introduced the optimization of a 3-phase composite, which included CNT, using the fibre volume fraction as the design variable. In the third optimization problem, two design variables were defined, fibre volume fraction and CNT weight fraction. The next optimization problem has 3 design variables, the fibre volume fraction, CNT weight fraction, and the fibre stacking angle. For the last design problem, the thickness of the layers in the composite were defined to be non-uniform and determined optimally. The problem was defined with 4 design variables, fibre volume fraction, CNT weight fraction, fibre stacking angle and the layer thickness ratio. The verification of the Ritz method for the vibration of the composite plate was conducted by comparing results with past literature and ANSYS. For the optimization technique, the accuracy of the solutions was compared using solutions from ANSYS.

CHAPTER 4 - RESULTS AND DISCUSSION

4.1 Introduction

This chapter presents the results for the optimization problems defined in chapter 3. Firstly, analysis results are presented which provide the motivation for the optimization study. This is followed by the detailed optimization results of the 8-layered laminate. The weight optimization problem for a simply supported plate is investigated for multiple design variables, subject to a frequency constraint using four parameters chosen as design variables. These variables were chosen since they have greater influence in improving the topology and stiffness of the composite, compared to parameters such as number of plies and shape of the plate. The results are obtained using MATLAB and the SQP optimization algorithm by varying the parameters and the design constraints mentioned previously. Weight optimization is conducted on both uniform and non-uniform layer thicknesses, and non-uniform distribution of reinforcement material in the composite. The use of carbon nanotubes and fibres in the composite is highlighted, where the 3-phase laminate motivates the aims of the research conducted. A discussion on the relationships between the parameters of the composite plate is made further in this chapter.

4.2 Analysis Results

Before introducing the optimization problems, an analytical investigation was carried out for the 2 and 3-phase composite plate. In Figure 4-1, the effect of adding CNTs to the composite is shown. Here the amounts of CNTs and fibre are assigned explicitly to show the influence of the reinforcement in the composite. A significant decrease in the non-dimensional weight is observed which indicates a more improved design for the composite plate. CNTs have showed to reduce the non-dimensional weight for all fibre angles and has provided a more consistent stiffness and non-dimensional weight as the fibre angle increased.

For a vibration response problem, and in this weight optimization problem in particular, the frequency plays a role in defining the problem and the performance potential for the composite plate. Shown in Figure 4-2 is the non-dimensional frequency, which is also used as the frequency constraint for the optimization problems. The results show a higher frequency response for every addition of CNT in the laminate and the optimal fibre stacking angle is closely to those achieved in Table 4-1, Table 4-2, and Table 4-3, which are presented later in this chapter. Essentially, the CNT reduces the difference between the non-dimensional weight for each fibre angle and gives a more consistent result/frequency for the different fibre angles. Table 4-1 provides the optimal fibre angles for the laminate with predefined values for CNT and fibre. Here, it also shows the maximum frequency and minimum weight which is found at those optimal points.

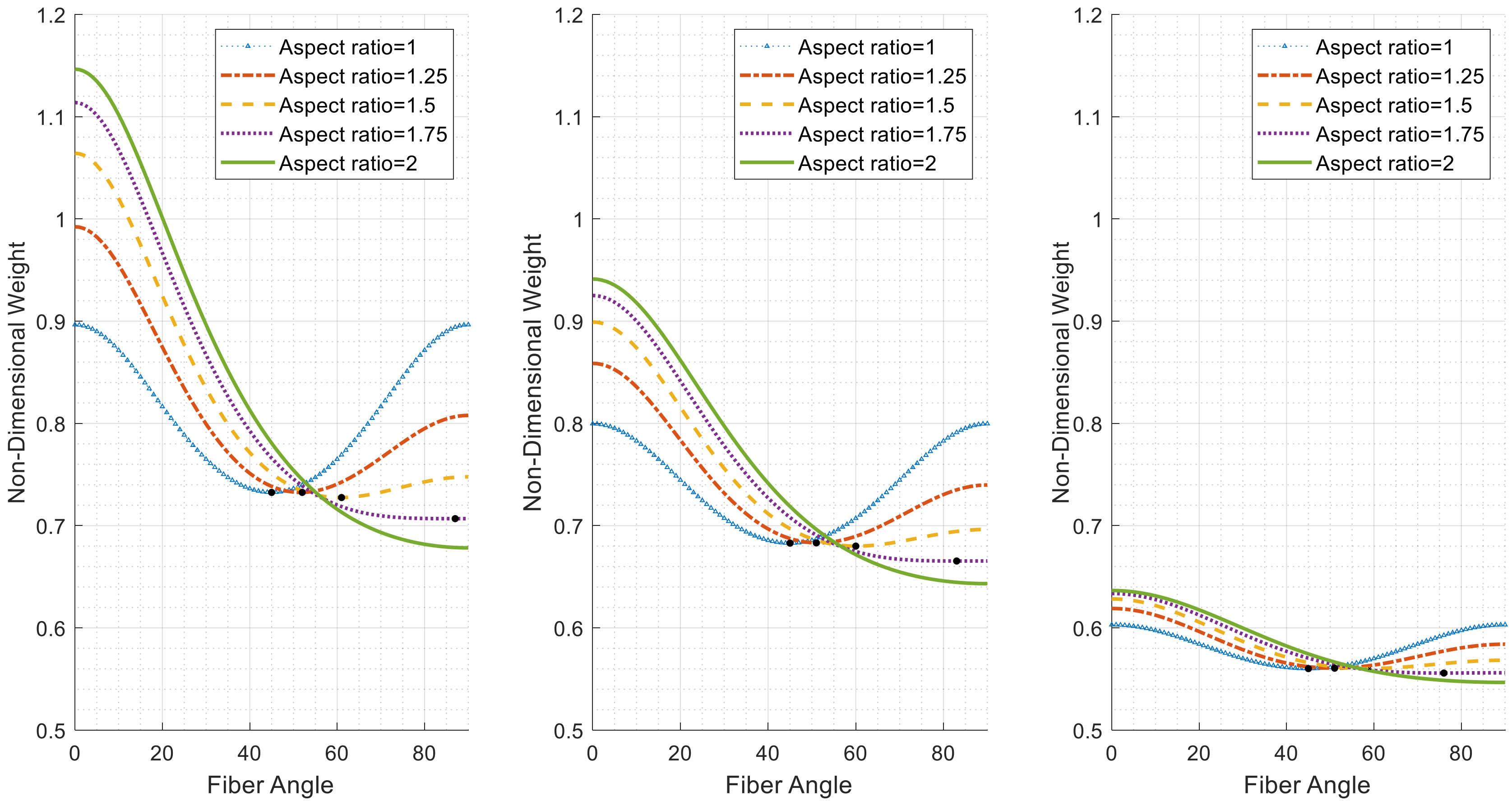

Figure 4-1: Non-dimensional weight vs fibre angle for a composite plate showing the addition of CNT reinforcement incrementally (Left: 30%fibre+0%CNT; Centre: 30%fibre+1%CNT; Right: 30%fibre+5%CNT)

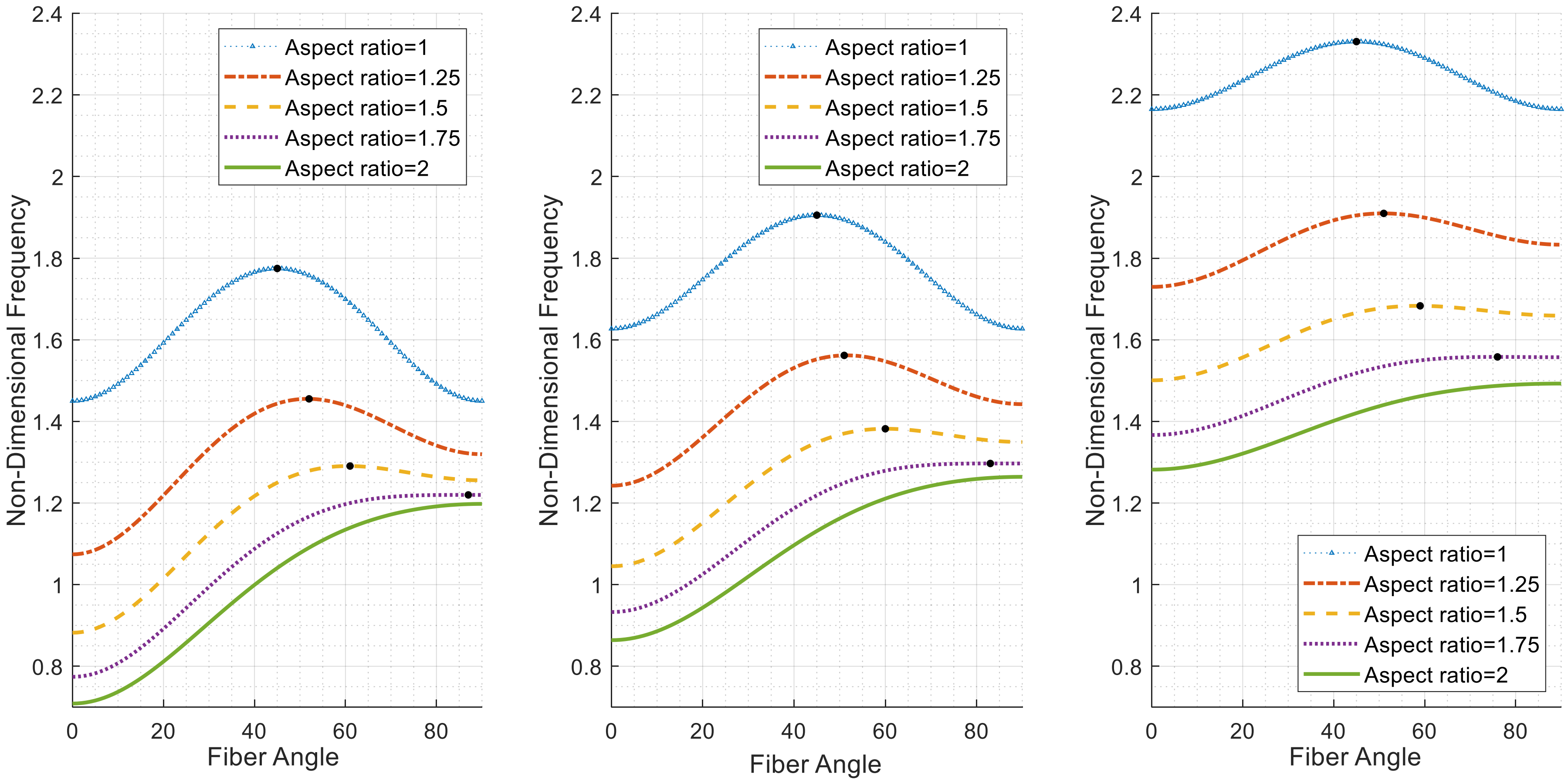

Figure 4-2:Non-dimensional frequency vs fibre angle for a composite plate showing the addition of CNT reinforcement incrementally (Left: 30%fibre+0%CNT; Centre: 30%fibre+1%CNT; Right: 30%fibre+5%CNT)

Table 4-1:Non-dimensional quantities showing results for CNT and fibre assigned explicitly

Aspect Ratio	V_f per layer	W_{CNT} per layer	Optimal Fiber Angle	Max. Non-Dimensional Frequency	W_L	W_0	Min. Non-Dimensional Weight
1	[0.3/ 0.3/ 0.3/ 0.3]s	[0.0/ 0.0/ 0.0/ 0.0]s	45	1.7747	15.6000	21.2968	0.7325
1.25			52	1.4552	19.5000	26.6202	0.7325
1.5			61	1.2906	23.4000	32.1652	0.7275
1.75			87	1.2199	27.3000	38.6226	0.7068
2			90	1.1979	31.2000	45.9980	0.6783
1	[0.3/ 0.3/ 0.3/ 0.3]s	[0.01/ 0.01/ 0.01/ 0.01]s	45	1.9053	15.6133	22.8637	0.6829
1.25			51	1.5617	19.5167	28.5684	0.6832
1.5			60	1.3819	23.4200	34.4413	0.6800
1.75			83	1.2969	27.3234	41.0625	0.6654
2			90	1.2642	31.2267	48.5441	0.6433
1	[0.3/ 0.3/ 0.3/ 0.3]s	[0.05/ 0.05/ 0.05/ 0.05]s	45	2.3306	15.6670	27.9674	0.5602
1.25			51	1.9097	19.5838	34.9333	0.5606
1.5			59	1.6831	23.5006	41.9491	0.5602
1.75			76	1.5580	27.4173	49.3286	0.5558
2			90	1.4926	31.3341	57.3175	0.5467

4.3 Optimization results

4.3.1 Problem 1: 2-Phase Uniform Layer Thickness and Non-Uniform Distribution of Reinforcement Material (Design variable: V_F)

In this optimization problem, the minimum weight is optimized using the fibre volume content as the single design variable and a graph of the optimal weight with respect to each fibre stacking angle and aspect ratio for the laminate is developed. Thus, Figure 4-3 shows the relationship between the fibre angle for different aspect ratios which indicated the optimal minimum weight for the laminate. As illustrated in Figure 4-3, the optimal stacking angle for all layers is 45° for a square laminate (aspect ratio=1) and increases towards 90° as the aspect ratio (a/b) reaches closer to 2. Table 4-2 provides the optimal solution for the distribution of fibre in the laminate and the optimal fibre angle for all the layers, with 1.3 as the frequency constraint and a constant thickness.

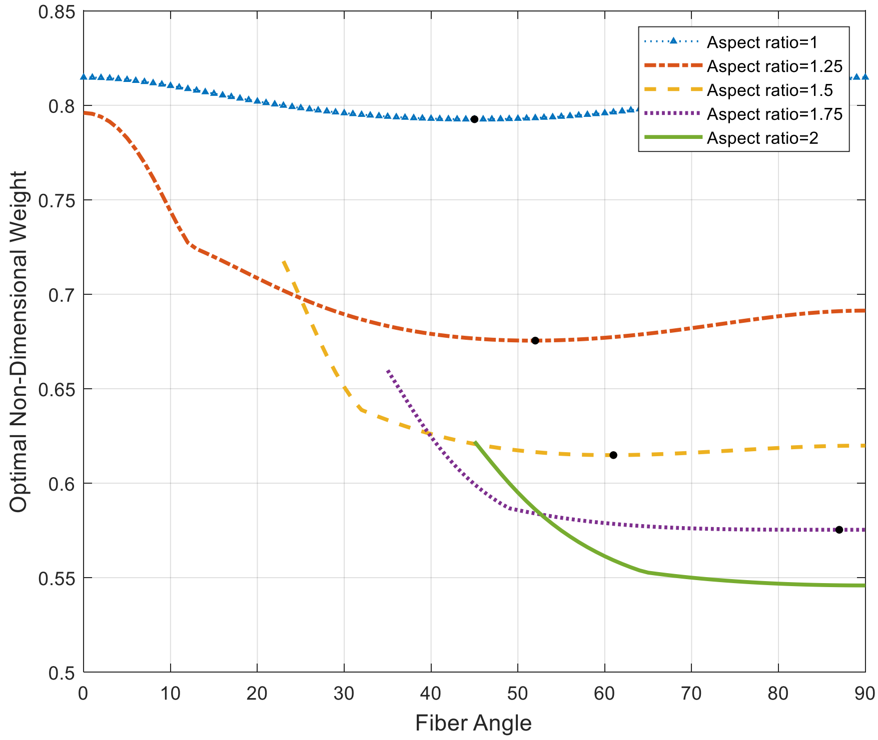

Figure 4-3: Optimal Non-Dimensional weight vs Fibre stacking angle for a 2-Phase laminate H=0.01; 0≤Vf≤0.6; Aspect ratio= a/b; f=1.3

Table 4-2: Optimal fibre angle and optimal Non-dimensional weight for 2-Phase laminate. H=0.01; $0 \le V_f \le 0.6$; Aspect ratio= a/b; f=1.3

Aspect Ratio	Optimal V_f per layer	Optimal Fiber Angle	W_L	W_0	Optimal Non-Dimensional Weight
1	[0.12/0/0/0]s	45	12.3647	15.6000	0.7926
1.25	[0.28/0/0/0]s	52	16.0627	23.7805	0.6755
1.5	[0.43/0/0/0]s	61	19.9214	32.4000	0.6149
1.75	[0.51/0/0/0]s	87	26.6813	41.1600	0.5753
2	[0.48/0/0/0]s	90	27.2503	49.9200	0.5459

According to the results presented for the 2-Phase laminate, the optimal fibre stacking angle is dependent on the aspect ratio and correlates with the results from previous literatures as well (Adali and Verijenko, 2001, Ehsani and Rezaeepazhand, 2016, Narita, 2003). For the distribution of the fibre content in the laminate, the optimal design is achieved by assigning a greater percentage of fibre/reinforcement material in the outer layers in order to satisfy the desired frequency constraint. The exterior layers contribute more to the overall stiffness of the laminate compared to the interior layers. This ensured that the required stiffness is achieved by simultaneously considering the stacking angles for each ply.

4.3.2 Problem 2: 3-Phase Uniform Layer Thickness and Non-Uniform Distribution of Reinforcement Material (Design variable: V_F)

For the next optimization problems, the carbon nanotubes are introduced in the composite which showed to have a high impact on the design efficiency factor. The high strength to weight ratio of the carbon nanotubes have a high influence on the minimum weight satisfying a frequency constraint, as indicated by the comparison of the optimal weight of the reinforced plate and the unreinforced reference isotropic plate. This comparison, results in a lower ratio which indicated a more efficient optimal weight design. This is illustrated in Figure 4-4.

A clear comparison can be made with Figure 4-3 and Figure 4-4 when CNTs are added to the weight optimization problem. For a frequency constraint for 1.3, which is used in both cases, the optimal non-dimensional weight is improved by adding CNT to the design. This reduces the amount of fibre reinforcement in the composite plate, which provides a lower weight while having the same frequency resistence. In Figure 4-4 (right), no solution was found for a/b=1 since the frequency constraint (=1.3) was not satisfied by the addtion of 2% CNT to the composite design.

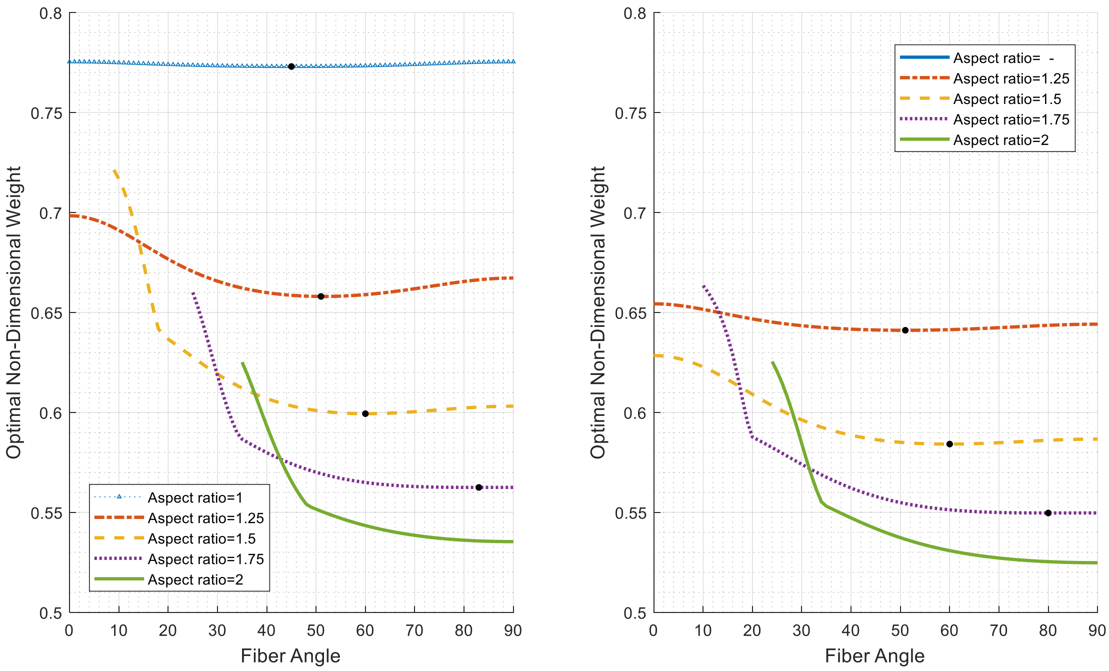

Figure 4-4: Optimal Non-dimensional weight vs Fibre stacking angle for a 3-Phase laminate H=0.01; $0 \leq V_f \leq 0.6$; Aspect ratio= a/b; f=1.3; W_{CNT}=1%(LEFT) ; W_{CNT}=2%(RIGHT)

The design parameters comprise of a frequency constraint being 1.3, a constant thickness H=0.01, an upper limit of 60% fibre volume fraction for each layer in the composite plate, and CNT weight fractions assigned explicitly for the respective solutions presented. The addition of CNTs in the composite has added extra stiffness and has enhanced the overall properties of the laminate, as mentioned earlier. This enhancement resulted in a higher design efficiency and has also affected the optimal fibre angle for the respective aspect ratios for the laminate in context. Table 4-3 highlights the detailed results for the 3-phase laminate consisting of 1% CNT in the overall laminate. By comparing the results from Table 4-2 and Table 4-3, the addition of CNT has reduced the volume fraction of fibre needed, which reduced the overall weight of the plate. The optimal fibre angle has reduced for some aspect ratios due to the smaller amount of fibre present from the optimization process.

Table 4-3:Optimal fibre angle and optimal Non-dimensional weight for 3-Phase laminate. H=0.01; $0 \le V_f \le 0.6$; Aspect ratio= a/b; f=1.3; W_{CNT}=1%

Aspect Ratio	Optimal V_f per layer	W_{CNT} per layer	Optimal Fiber Angle	W_L	W_0	Optimal Non-Dimensional Weight
1	[0.015/0/0/0]s	[0.01/0.01/0.01/0.01]s	45	12.0583	15.6000	0.7730
1.25	[0.17/0/0/0]s	[0.01/0.01/0.01/0.01]s	51	15.6470	23.7805	0.6580
1.5	[0.31/0/0/0]s	[0.01/0.01/0.01/0.01]s	60	19.4187	32.4000	0.5993
1.75	[0.4/0/0/0]s	[0.01/0.01/0.01/0.01]s	83	23.1512	41.1600	0.5625
2	[0.45/0/0/0]s	[0.01/0.01/0.01/0.01]s	90	26.7245	49.9200	0.5353

Table 4-4 includes the optimal quantities for the 3-phase laminate consisting of 2% CNT in the overall laminate. This shows a similar improvement of the design efficiency and fibre angles as mentioned previously. The main objective for the optimization problem is to ensure that the weight optimization is carried out with the design constraints introduced and all constraints being satisfied. This is successfully achieved for the frequency constraint of 1.3 using the fibre volume content as the design variable and it has shown that the optimal solution is improved by adding CNTs to the design.

Table 4-4:Optimal fibre angle and optimal Non-dimensional weight for 3-Phase laminate. H=0.01; $0 \le V_f \le 0.6$; Aspect ratio= a/b; f=1.3; W_{CNT}=2%

Aspect Ratio	Optimal V_f per layer	W_{CNT} per layer	Optimal Fiber Angle	W_L	W_0	Optimal Non-Dimensional Weight
1	-	[0.02/0.02/0.02/0.02]s	-	-	-	-
1.25	[0.06/0/0/0]s	[0.02/0.02/0.02/0.02]s	51	15.2447	23.7805	0.6411
1.5	[0.2/0/0/0]s	[0.02/0.02/0.02/0.02]s	60	18.9260	32.4000	0.5841
1.75	[0.3/0/0/0]s	[0.02/0.02/0.02/0.02]s	80	22.6247	41.1600	0.5497
2	[0.36/0/0/0]s	[0.02/0.02/0.02/0.02]s	90	26.1975	49.9200	05248

4.3.3 Problem 3: 3-Phase Uniform Layer Thickness and Non-Uniform Distribution of Reinforcement Material (Design variables: V_F and W_{CNT})

In this optimization problem, there are 2 design variables which will be used to determine the minimum weight of the composite. Due to the increase in design variables, there would be multiple optimal values for the minimum weight due to the combined effects of CNT and fibre and the varying amounts of the two reinforcement materials when used in the composite.

In Figure 4-5, multiple optimal values are achieved for a square laminate (aspect ratio=1). From previous results, it is known that the optimal fibre angle is 45° for square laminates hence, 45° was used for all the layers in the figure below. Here, the values in the surface layer are shown since these layers gives a higher contribution to the stiffness of the plate. A frequency constraint of 1.75 was specified for this solution with a constant laminate thickness H=0.01. At 0% fibre volume fraction in the surface layer, multiple minimum values are achieved, for CNT weights of 2% to 5% in the surface layers. This is due to the interior layers being optimized and adjusting the amount of reinforcement in the layers to provide the same optimal solution using the fixed frequency constraint. For the surface layers with CNT content below 2% and fibre below 10%, the weight is higher. This is a result of the surface layers not being adequately reinforced, hence having more reinforcement in the interior layers of the laminate so that the design constraints are met for the optimization.

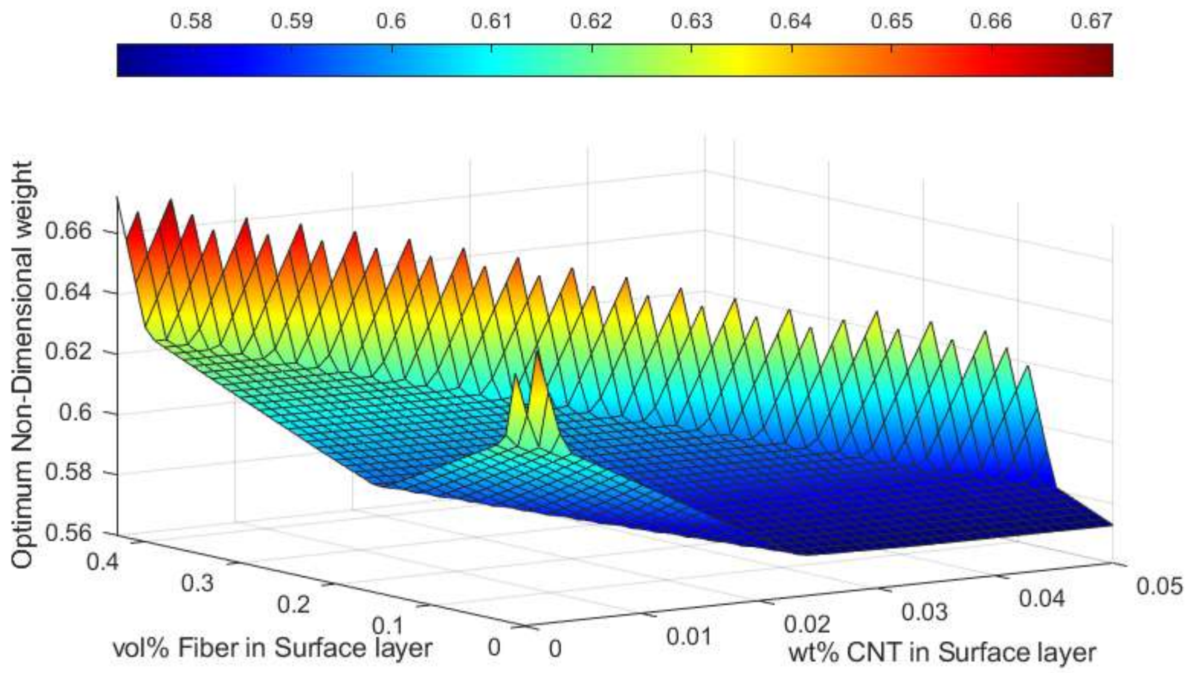

Figure 4-5: Surface plots for the 3-Phase square laminate showing the volume fraction and weight fraction of CNT and glass fibres in the surface layers; H=0.01; $0 \leq V_{fi} \leq 0.6$; $0 \leq W_{CNTi} \leq 0.05$; a/b= 1; f=1.75

The solution in Figure 4-5 is a single solution showing the optimal results for a frequency constraint of 1.75 with a constant laminate thickness H=0.01. To gain a wider understanding of the optimization problem, and the way in which the solution is gained, many optimization problems had to be solved with each having updated input parameters and constraints. In Figure 4-6, several optimization problems with increasing values of the frequency constraint are solved, with 2 design variables, the fibre and CNT content. In this figure, the optimal quantities of the reinforcement materials are shown per layer as the frequency constraint increases. The fibre volume content was constrained at 60% per layer and the CNT weight content limited at 5% per layer. The diagrams indicate that for low frequencies, until the value of 1.65, no fibres are introduced, and the target of minimum weight is achieved by using non-zero CNT reinforcement. This is due to the optimization algorithm which optimizes the quantities of reinforcement material according to the ability of it to converge to the optimum solution more easily. To achieve higher frequency constraints, fibre reinforcement is added in the surface layer and the CNT content remains at maximum for the surface layer.

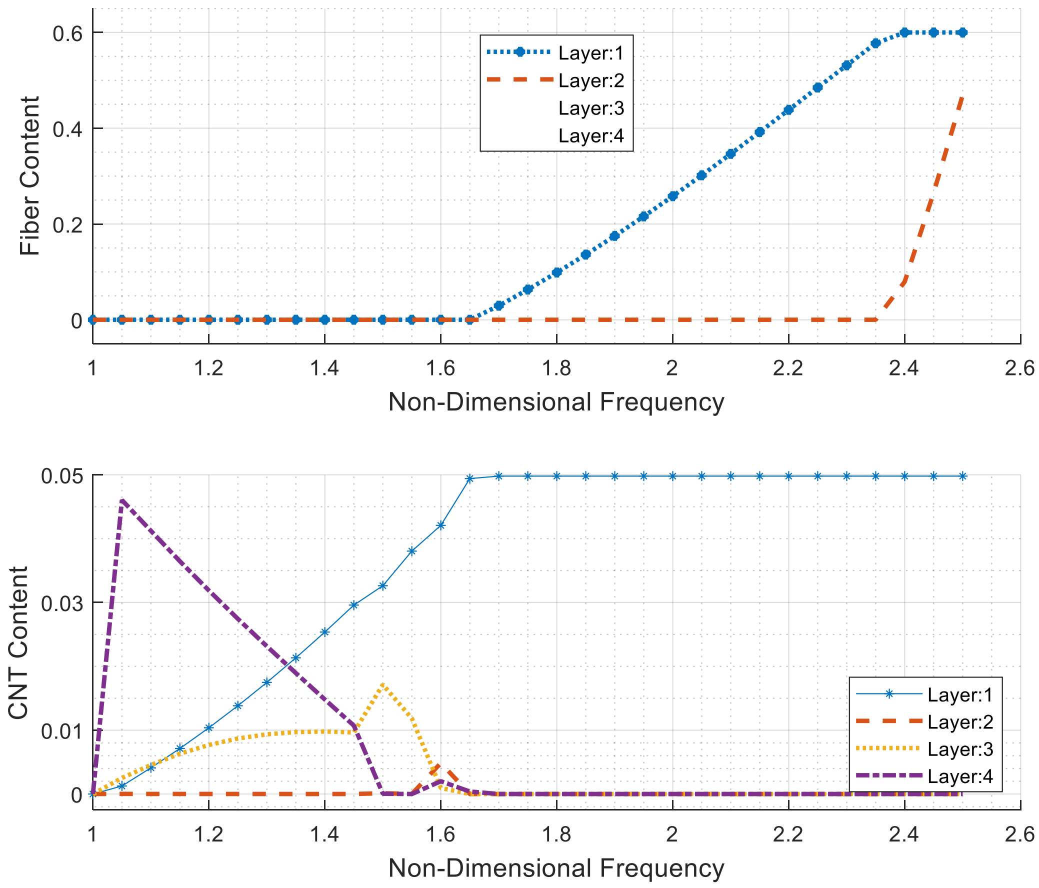

Figure 4-6: Fibre and CNT reinforcement per layer versus non-dimensional frequency

In the figure that follows, the relationships between the non-dimensional frequency and the weight variables of composite plate and the reference plate is presented. Figure 4-7 shows 3 graphs: a) Optimal non-dimensional weight (=design efficiency factor) vs frequency, b) Optimal weight vs frequency, and c) Optimal weight of reference plate vs frequency. Diagram a) shows the decrease of the optimal non-dimensional weight for increased frequencies. Diagram b) shows an increase of optimal weight for increased frequency, and diagram c) shows increase of optimal weight for the reference plate for increased frequency. Ideally, it would be expected that the increase of the frequency would result in an increase of the optimal non-diimensional weight (reduced design efficiency), since higher frequencies results in higher amounts of reinforcement for the composite. But, the formulation of the non dimensioal quantities is very interesting with respect to the reference plate. For the reinforced composite plate with a constant thickness (H), as the frequency increases, the weight of the composite also increases, as more reinforcement is added. However, for the reference isotropic plate, for the specified frequency constraint, there is no reinforcement in the plate therefore, the thickness of the isotropic plate increases. The added thickness increases the weight of the isotropic plate in order to satisfy the frequency contraint and therefore meeting the optimization requirements. The figure summarises that as the frequency constraint increases, the expected weight of the laminate should also increase but not as much as the weight of the reference plate. Hence the improvement in the design by adding CNT and fibre reinforcement.

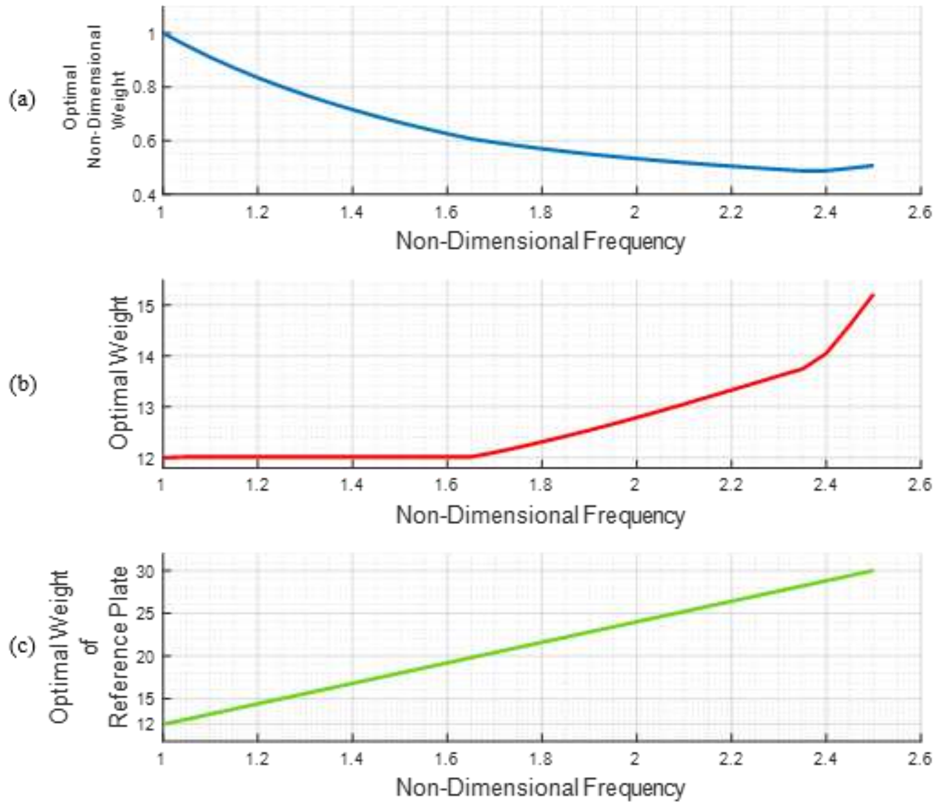

Figure 4-7: Graphs showing the optimized quantities for the specified frequency constraints for an 8-layered laminate subject to H=0.01; $0 \leq V_{fi} \leq 0.6$; $0 \leq W_{CNTi} \leq 0.05$; a/b= 1; θ=45°

Next, in Figure 4-8 an attempt is made to provide the influence of stacking sequence, on the min-weight optimization problem. Several optimization problems with frequency constraint = 1.5 are solved for a square laminate, with one design variable, the CNT content. The fibre content is considered equal for every layer and varies along the x axis of each diagram. Figure 4-8 (a to d) are obtained for different stacking sequence, with fibre angles equal to 0, 15, 30, and 45 degrees, for every layer in each subfigure respectively. Figure 4-8 shows that although for zero fibre reinforcement the same non-dimensional min-weight is obtained, for gradually increased fibre content, the increase of fibre angle from a to d results in the clear decrease of the optimal weight, expressing the influence of the stacking sequence. Thus, as fibre angles of every layer approach 45 degrees, the optimal weight decreases respectively.

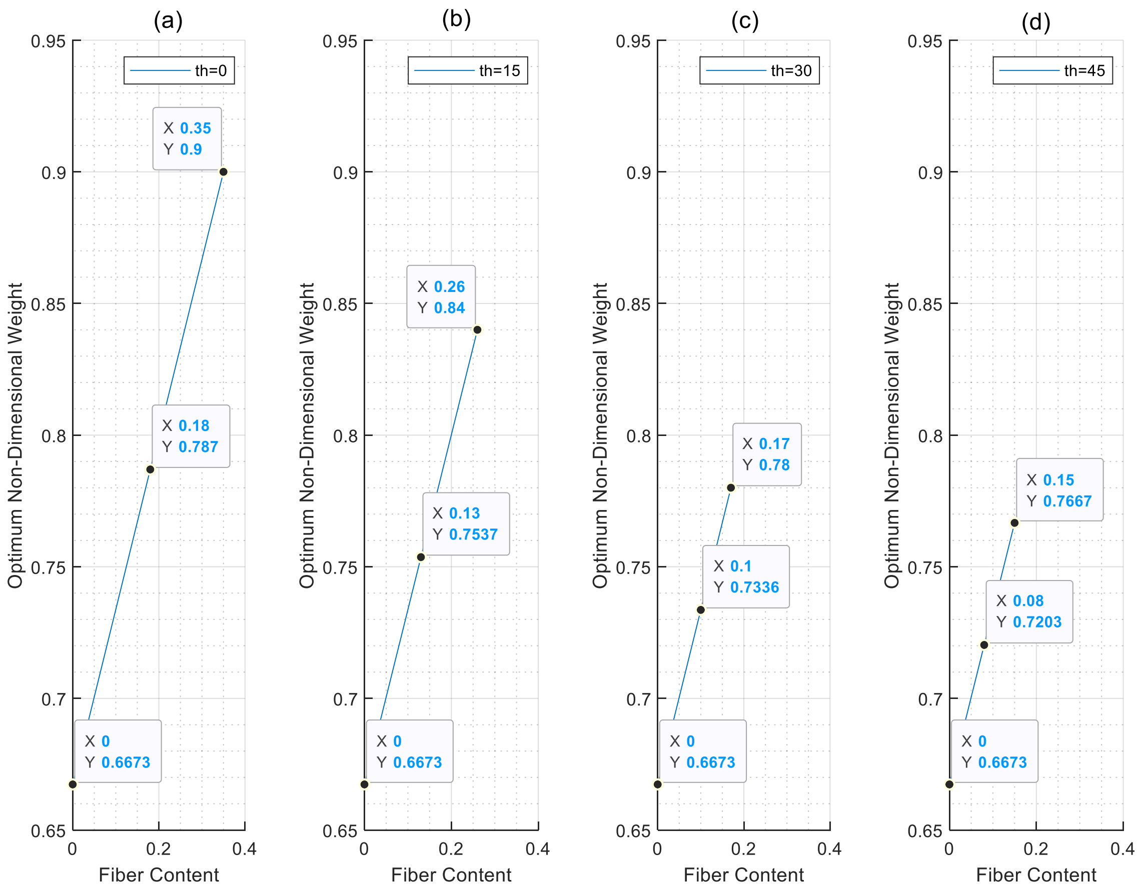

Figure 4-8: Optimum Non-dimensional weight vs %Vol. Fibre Content for 3-phase laminate

Table 4-5 shows the representative solutions for the optimization problems which have been solved to produce diagrams of Figure 4-8. According to Table 4-5, as the fibre content is increased explicitly (outside optimization) for every layer, the CNT content which arises from the optimization solution decreases in order to meet the frequency constraint and the optimal weight increases. Thus, more fibre content and less CNT content results in increased weight, indicating that CNT has a greater effect on the weight minimization problem, compared to fibres. Regarding the fibre angle, this graph verifies the results in Figure 4-1, Figure 4-3, and Figure 4-4, which says that the Minimum ratio or Optimum Non-dimensional weight is achieved at 45° degrees for a square plate.

Table 4-5: Detailed solution to the diagrams in Figure 4-8

Fiber Angle	V_f per layer	W_{CNT} per layer	Non-Dimensional Frequency	W_L	W_0	Non-Dimensional Weight
0	[0.0/ 0.0/ 0.0/ 0.0]s	[0.032/ 0/ 0/ 0]s	1.5	12.0120	18	0.6673
0	[0.18/ 0.18/ 0.18/ 0.18]s	[0.014/ 0/ 0/ 0]s	1.5	14.1654	18	0.7870
0	[0.35/ 0.35/ 0.35/ 0.35]s	[0.0002/ 0/ 0/ 0]s	1.5	16.2001	18	0.9
15	[0/ 0/ 0/ 0]s	[0.032/ 0/ 0/ 0]s	1.5	12.0120	18	0.6673
15	[0.13/ 0.13/ 0.13/ 0.13]s	[0.015/ 0/ 0/ 0]s	1.5	13.5658	18	0.7537
15	[0.26/ 0.26/ 0.26/ 0.26]s	[0.0009/ 0/ 0/ 0]s	1.5	15.1203	18	0.84
30	[0.0/ 0.0/ 0.0/ 0.0]s	[0.032/ 0/ 0/ 0]s	1.5	12.0120	18	0.6673
30	[0.1/ 0.1/ 0.1/ 0.1]s	[0.013/ 0/ 0/ 0]s	1.5	13.2050	18	0.7336
30	[0.17/ 0.17/ 0.17/ 0.17]s	[0.0013/ 0/ 0/ 0]s	1.5	14.0405	18	0.7800
45	[0/ 0/ 0/ 0]s	[0.032/ 0/ 0/ 0]s	1.5	12.0120	18	0.6673
45	[0.08/ 0.08/ 0.08/ 0.08]s	[0.015/ 0/ 0/ 0]s	1.5	12.9655	18	0.7203
45	[0.15/ 0.15/ 0.15/ 0.15]s	[0.0004/ 0/ 0/ 0]s	1.5	13.8001	18	0.7667

Next, the advantage of the 3-phase CNT/fibre reinforced laminate in comparison to traditional, 2-phase fibre reinforced composite is highlighted, for optimization problems of different stacking sequences. Figure 4-9 provides the optimal solution for symmetric and anti-symmetric angled and cross ply stacking sequences subject to a frequency constraint of 1.75, for 2-phase and 3-phase square laminates. According to Figure 4-9, the optimal non-dimensional weight is significantly reduced for the 3-phase laminate, for every stacking sequence. This reduction indicates that the design efficiency is increased respectively, for 3-phase laminates, comparing to 2-phase fibre reinforced composites. The quantities of fibre and CNT in each layer were limited to 60% volume fraction and 5% weight fraction respectively.

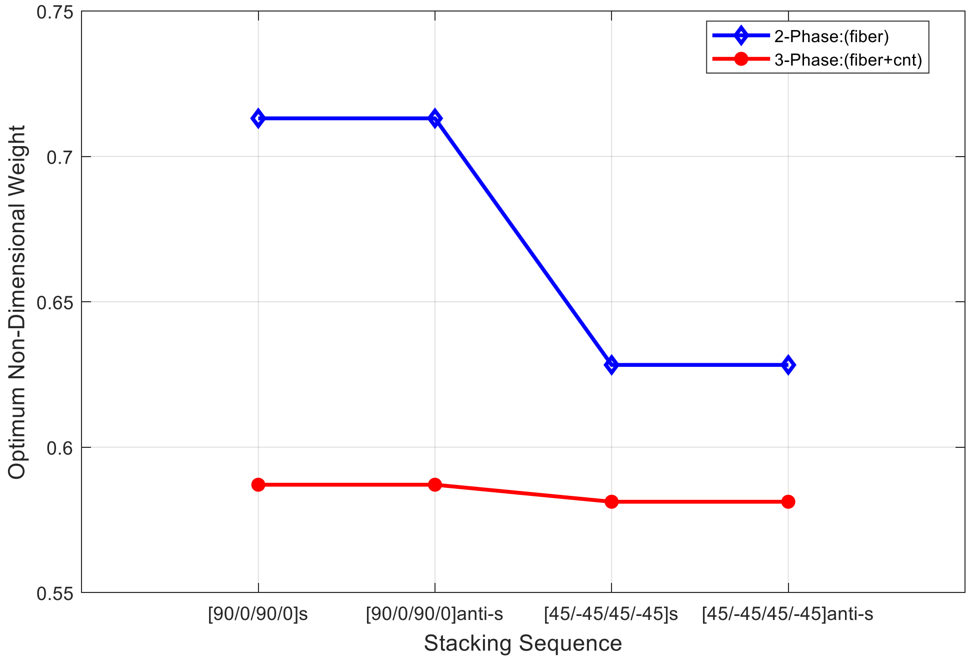

Figure 4-9: Optimum Minimum Weight vs Different Stacking sequences for 2-Phase and 3-Phase laminate; subject to H=0.01; $0 \le V_{fi} \le 0.6$; $0 \le W_{CNTi} \le 0.05$; W_{CNTmax}=1.25%; a/b=1; f=1.75

Table 4-6 gives the optimal design quantities for the 2-phase and 3-phase laminate results using a frequency constraint of 1.75 as illustrated in Figure 4-9. As expected, there are higher amounts of reinforcement in the surface layers and a more improved design efficiency factor for the angled ply stacking configuration. The fibre volume fraction was limited to 60% per layer and the CNT weight fraction was limited to 5% per layer whilst having an overall CNT limit of 1.25% for the entire laminate. According to Table 4-6, the non-dimensional weight which represents the design efficiency factor is improved by [(0.7131-0.5870)/0.7131]x100 = 17.6% for cross-ply and [(0.6283-0.5812)/0.6283]x100 = 7.5% for angle ply laminates.

Table 4-6: Minimum weight design for 2-Phase and 3-Phase laminate with 8-layeres subject to H=0.01; $0 \le V_{fi} \le 0.6$; $0 \le W_{CNTi} \le 0.05$; W_{CNTmax}=1.25%; a/b=1; f=1.75 for different stacking sequences

2 Phase Laminate (Fiber only): Design variable = Fiber (BLUE LINE)					
Stacking Sequence	**V_f per layer**	**W_{CNT} per layer**	**W_L**	**W_0**	**Optimal Non-Dimensional Weight**
[90/0/90/90]s	[0.6/0.39/0/0]s	[0/0/0/0]s	14.9748	21.0	0.7131
[90/0/90/90]a-s	[0.6/0.39/0/0]s	[0/0/0/0]s	14.9748	21.0	0.7131
[45/-45/45-45]s	[0.4/0/0/0]s	[0/0/0/0]s	13.1941	21.0	0.6283
[45/-45/45-45]a-s	[0.4/0/0/0]s	[0/0/0/0]s	13.1941	21.0	0.6283
3 Phase Laminate(Fiber + CNT): Design variable = Fiber and CNT (RED LINE)					
Stacking Sequence	**V_f per layer**	**W_{CNT} per layer**	**W_L**	**W_0**	**Optimal Non-Dimensional Weight**
[90/0/90/0]s	[0.1/0/0/0]s	[0.05/0/0/0]s	12.3288	21.0	0.5870
[90/0/90/0]a-s	[0.1/0/0/0]s	[0.05/0/0/0]s	12.3288	21.0	0.5870
[45/-45/45-45]s	[0.06/0/0/0]s	[0.05/0/0/0]s	12.2059	21.0	0.5812
[45/-45/45-45]a-s	[0.06/0/0/0]s	[0.05/0/0/0]s	12.2059	21.0	0.5812

Considering the 3-phase 8-layered square laminate with uniform layer thickness, the effect from using CNTs in the composite is investigated further. From previous results, it is known that CNTs influence the overall stiffness in the laminate and allows for high design efficiency factors to be achieved. Looking at Figure 4-10, the surface plot shows how the total amount of CNT affects the overall stiffness of the laminate for fibre angles 0° to 90°. The frequency constraint of 1.75 was assigned so that a transparent solution could be shown for the 3-phase laminate. For 0% CNT in the overall laminate, a 2-phase laminate exists and the variation of optimum non-dimensional quantities at different fibre angles are very high. As the total amount of CNT is increased incrementally, up to 5% per layer, a significant reduction is observed in the difference of optimized weight values for every fibre stacking angle and they all show an optimum fibre value of 45°, which is expected for a square laminate. As noted from previous results, the addition of CNT to the 2-phase laminate improved the design efficiency on all levels and gave a more consistence result at all fibre angles.

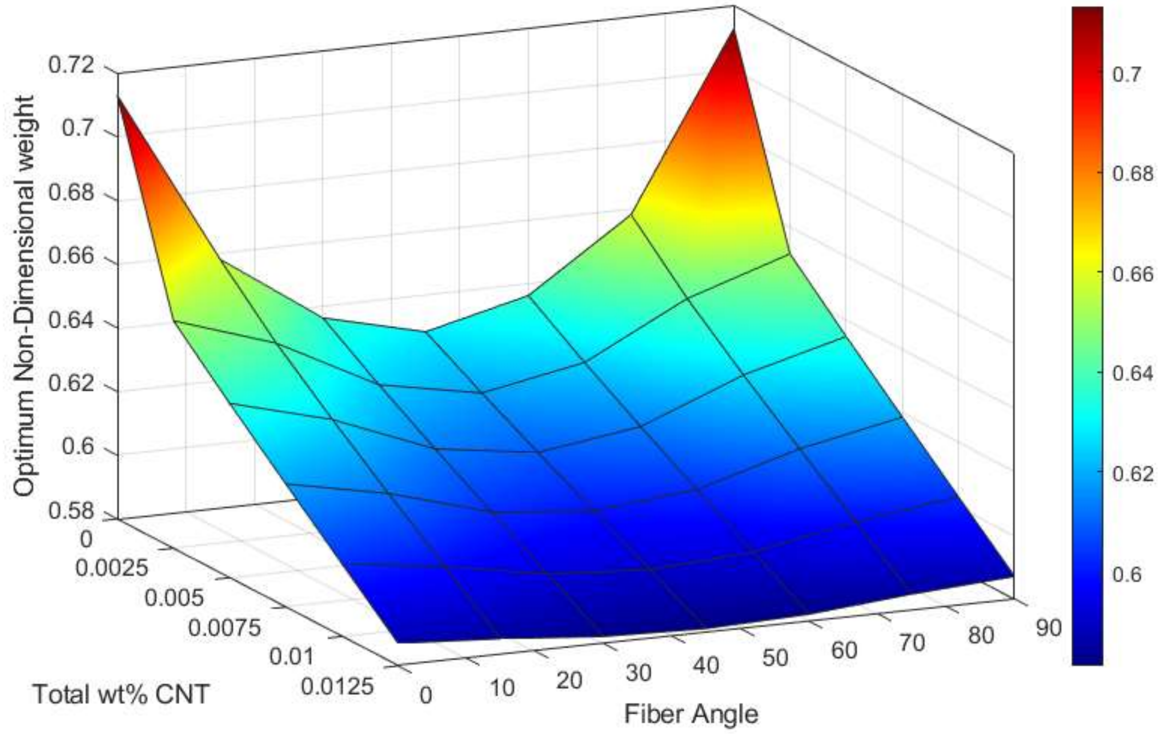

Figure 4-10: Surface plots for the 3-Phase square laminate showing the total weight % of CNT and the optimal fibre angle in all layers; subject to H=0.01; $0 \leq V_{fi} \leq 0.6$; $0 \leq W_{CNTi} \leq 0.05$; W_{CNTmax}=as shown; a/b= 1; f=1.75

4.3.4 Problem 4: 3-Phase Uniform Layer Thickness and Non-Uniform Distribution of Reinforcement Material (Design variables: V_F, W_{CNT}, fibre angle)

In this section, the optimization algorithm is carried out by introducing another design variable for the optimal design of the 3-phase hybrid composite plate. The fibre angle is the additional design variable for this optimization problem, and this is optimized along with the fibre content and CNT content in the composite plate.

From previous results, using one and two variables, the fibre stacking angle was constant for every layer and the results showed an optimal fibre angle of 45° for square laminates. This is taken a step further by finding the optimal fibre angle in each layer which then results in the optimal stacking sequence for the 8-layered laminate. To highlight the sensitivity of the results in respect to the frequency constraint, results of the problem with 3 design variables are presented in Table 4-7 for an increasing frequency constraint. For a proper indication of the outcome of these simulations, the optimal weight instead of the optimal non-dimensional weight is used. According to Table 4-7, for low frequency constraints, there are small to minimal amounts of fibres present in all the layers of the composite and the need to satisfy the frequency constrained is covered by CNT reinforcement only. As the frequency constraint increases, the amount of fibre reinforcement also increases with more reinforcement placed in the surface layers of the laminate. Results also showed that the outer layers of the laminate contributed most to the stiffness of the laminate. Using this information, the optimal fibre angle in the outer layers is 45°, which corresponds to the optimal fibre angle for square laminates. For the inner layers, the optimal values increase towards 45° as the frequency constraint increases as well.

To highlight the advantage of the optimization with 3 design variables, a comparison with results obtained with one design variable (fibre content) given in Table 4-3 is considered, for increasing aspect ratios. An increase in the design efficiency, translated as decrease of the optimal non-dimensional weight is observed in Table 4-8, in comparison to Table 4-3. This increase varies between 0.4% and 3.5% for the different aspect ratios. The benefit of using the model with 3 design variables is better highlighted, if it is noticed that for all aspect ratios, Table 4-8 depicts significantly lower content of fibres comparing to Table 4-3, with the same total amount of CNT. Thus, the reduction of the weight is accompanied by a reduction in the cost, resulting in a cost-effective design.

Table 4-7: Minimum weight design for 3-Phase laminate with 8-layers subject to 3 design variables H=0.01; $0 \leq V_{fi} \leq 0.6$; $0 \leq W_{CNTi} \leq 0.05$; W_{CNTmax}=1.25%; $-90 \leq \theta \leq +90$; a/b=1

Frequency Constraint	Optimal Fiber Angle	Optimal Vf per layer	Optimal W_{CNT} per layer	W_L Optimal weight	W_0 Reference weight	Optimal Non-Dimensional Weight
1.25	[45/ 30/ 30/ 45]s	[0/ 0/ 0/ 0]s	[0.009/ 0.011/ 0.007/ 0.023]s	12.017	15.0	0.801
1.3	[45/ 30/ 30/ 45]s	[0/ 0/ 0/ 0]s	[0.013/ 0/ 0.037/ 0]s	12.017	15.6	0.7703
1.5	[45/ 30/ 30/ 45]s	[0/ 0/ 0/ 0]s	[0.036/ 0/ 0/ 0.014]s	12.017	18.0	0.667
1.75	[45/ 45/ 30/ 45]s	[0.063/ 0/ 0/ 0]s	[0.05/ 0/ 0/ 0]s	12.206	21.0	0.581
2	[45/ 60/ 0/ 30]s	[0.26/ 0/ 0/ 0]s	[0.05/ 0/ 0/ 0]s	12.79	24.0	0.533
2.2	[45/ 0/ 0/ 30]s	[0.44/ 0/ 0/ 0]s	[0.05/ 0/ 0/ 0]s	13.33	26.4	0.505
2.4	[45/ 45/ 30/ 45]s	[0.6/ 0.08/ 0/ 0]s	[0.05/ 0/ 0/ 0]s	14.055	28.8	0.488
2.5	[45/ 45/ 90/ 45]s	[0.6/ 0.47/ 0/ 0]s	[0.05/ 0/ 0/ 0]s	15.2239	30.0	0.5075

Table 4-8: Optimal fibre angle and optimal Non-dimensional weight for 3-Phase laminate. H=0.01; $0 \leq V_f \leq 0.6$; $0 \leq W_{CNTi} \leq 0.05$; W_{CNTmax}=1%; $-90 \leq \theta \leq +90$; Aspect ratio= a/b; f=1.3

Aspect Ratio	Optimal Fiber Angle	Optimal Vf per layer	Optimal W_{CNT} per layer	W_L Optimal weight	W_0 Reference weight	Optimal Non-Dimensional Weight
1	[45/45/0/45]s	[0/0/0/0]s	[0.015/0/0.025/0]s	12.013	15.6	0.7701
1.25	[45/30/30/45]s	[0.023/0/0/0]s	[0.04/0/0/0]s	15.1036	23.7805	0.6351
1.5	[60/45/0/45]s	[0.17/0/0/0]s	[0.04/0/0/0]s	18.76	32.4	0.579
1.75	[90/90/0/45]s	[0.28/0/0/0]s	[0.04/0/0/0]s	22.47	41.16	0.5459
2	[90/0/0/45]s	[0.34/0/0/0]s	[0.04/0/0/0]s	26.073	49.92	0.522

4.3.5 Problem 5: 3-Phase Non-Uniform Layer Thickness and Non-Uniform Distribution of Reinforcement Material (Design variables: V_F, W_{CNT}, fibre angle, thickness ratio)

This set of numerical results presents the optimal design for the 3-phase hybrid composite plate using four design variables in the optimization algorithm. For this problem, the non-uniform layer thickness is investigated for all the layers in the composite plate. The layer thickness ratio is taken as the ratio of the thickness of each layer (**h**) and the thickness of the overall plate (**H**). For this final investigation, the optimal quantities of fibre content, CNT content, fibre angles and thickness ratios are shown in Table 4-9 for a square laminate for multiple frequency constraints.

From observation, zero fibre content is obtained for low frequency constraints and higher CNT content appears in interior layers. For higher frequency constraints, higher content of fibre and CNT reinforcement as well as higher thickness ratios are obtained for the outer layers. The thicker outer layers at high frequencies are suitable to provide the necessary stiffness to the overall composite plate which satisfies the frequency constraint.

The benefit of using a varying thickness on weight optimization is highlighted, by a comparison of Table 4-7, with 3 design variables (fibre and CNT content, fibre angle) and uniform thickness, and Table 4-9, with 4 design variables and varying thickness for a square plate. The design efficiency as expressed by the optimal non-dimensional weight, is gradually improved for increasing frequency constraints in the problem with 4 design variables. For the first three values of frequency constraint, the same design efficiency is obtained from the problem of 3 and 4 design variables, attributed to the zero-fibre content. However, for higher frequency constraints, the optimization problem with 4 design variables(Table 4-9), depicts an increase in the design efficiency comparing to the problem with 3 design variables(Table 4-7), equal to 1.2%, 1.7%, 2%, 3.1% and 6.9% for increasing values of the frequency constraint 1.75 to 2.5. Thus, as the need for higher frequency constraints appears, the benefit from lower weight increases when non-uniform thickness is considered in the optimization process.

Finally, comparison between Table 4-7 and Table 4-9 indicates that for the last (and highest) frequency constraints, the quantity of the fibre content is lower for the case of optimization with non-uniform thickness. This results in the cost-effective design of the laminate, which simultaneously satisfies the minimum weight criterion. The use of multiple design variables allow for a better optimized result since many parameters of the composite is being assigned optimally.

Table 4-9: Minimum weight design for 3-Phase laminate with 8-layers subject to 4 design variables, H=0.01; $0 \le V_{fi} \le 0.6$; $0 \le W_{CNTi} \le 0.05$; W_{CNTmax}=1.25%; $-90 \le \theta \le +90$; $0.01 \le h/H \le 0.15$; a/b=1; $\sum_{i=1}^{8} \frac{h_i}{H} = 1$

Frequency Constraint	Optimal Fiber Angle	Optimal Vf per layer	Optimal W_{CNT} per layer	Thickness ratio h/H	W_L Optimal weight	W_0 Reference weight	Optimal Non-Dimensional Weight
1.25	[45/30/30/45]s	[0/0/0/0]s	[0.005/0.019/0.018/0.01	[0.15/0.15/0.1/0.1]s	12.017	15	0.8011
1.3	[45/30/30/45]s	[0/0/0/0]s	[0.005/0.027/0.015/0.003]s	[0.15/0.15/0.1/0.1]s	12.017	15.6	0.7703
1.5	[45/30/30/45]s	[0/0/0/0]s	[0/0.04/0/0.01]s	[0.05/0.15/0.15/0.15]s	12.017	18	0.667
1.75	[45/0/30/30]s	[0.15/0/0/0]s	[0.05/0/0/0]s	[0.15/0.15/0.1/0.1]s	12.063	21	0.574
2	[45/45/60/45]s	[0.19/0/0/0]s	[0.05/0/0/0]s	[0.15/0.15/0.06/0.14]s	12.58	24	0.524
2.2	[45/90/90/30]s	[0.35/0/0/0]s	[0.05/0/0/0]s	[0.15/0.15/0.1/0.1]s	13.075	26.4	0.495
2.4	[45/45/45/30]s	[0.53/0/0/0]s	[0.05/0/0/0]s	[0.15/0.12/0.09/0.14]s	13.614	28.8	0.4727
2.5	[45/45/30/45]s	[0.6/0.13/0/0]s	[0.05/0/0/0]s	[0.15/0.13/0.08/0.14]s	14.2052	30	0.4735

4.4 Summary

In this chapter, the results for the weight optimization were presented. The motivation for using nanomaterials as reinforcement in the composite plate was shown. The optimization problems defined in chapter 3 were successfully conducted using MATLAB and the SQP algorithm, with the respective design variables and constraints. For each optimization problem, the weight optimization was achieved, and optimal parameters of the composite plate were shown. The effect of CNTs in the 3-phase laminate was investigated and the benefits of using optimization to minimise material use was highlighted.

From the results for the optimization problems, the optimal fibre angles for square laminates were found to be at 45°. As the aspect ratio of rectangular plates increase towards 2, the optimal fibre angle increases towards 90°. There showed to be a higher design efficiency for high frequency constraints, showing up to 51.2% improvement (=1-0.488) in the non-dimensional weight at a frequency constraint of 2.4, by incorporating CNTs and optimization parameters with two and three design variables. The design variables influenced the weight optimization results as the number of design variables increased, which showed to be 52.7% improvement (=1-0.4727) in the non-dimensional weight for composites with non-uniform layer thickness, using four design variables at a frequency constraint of 2.4. The inclusion of the fibre stacking angle and the layer thickness ratio as design variables in the optimization problem has improved the weight optimization approach. This allowed for more parameters of the composite plate to be determined optimally, which resulted in an overall efficient design.

CHAPTER 5 - CONCLUSION & RECOMMENDATIONS

5.1 Conclusion

In this study, the optimal lightweight design of a hybrid, CNT/fibre reinforced composite laminate, subject to a frequency constraint, was presented. The use of multi-scale and multiphase reinforcements was applied to the 8-layered composite plate and weight optimization problems were developed.

A literature review was successfully conducted by gathering relevant research which formed a foundation to the theoretical background to this study. Material science and engineering methods, using the Halpin-Tsai equations and fibre micromechanics were implemented, to obtain the effective properties of the 3-phase composite plate. Past research and mathematical equations helped formulate the natural vibration problem, which were solved analytically using the Ritz method, for the simply supported (SSSS) boundary condition. A review on optimization algorithms and applications provided great insight on the optimization techniques used for composite designs. The optimization design of the composite plate was effectively implemented using a Sequential Quadratic Programming (SQP) algorithm which was modelled using MATLAB software, integrating the micromechanics and the vibration analysis problem for the lightweight design of the composite plate.

A verification of the vibration analysis method was conducted by comparing against numerical results from published sources and commercial software (ANSYS), resulting in an exceptional agreement in results for this present study. The verification process also gave great confidence with the optimization algorithm and implementation of the optimum design. This was conducted by comparing results with numerical methods (FEM and ANSYS), which showed a good trend of results that complimented the optimization methods used for the composite design. From the discussions made, the aims and objectives of this study has been successfully achieved.

The purpose of this study was to gain sufficient knowledge to provide answers to the research question:

What effect does the parameters and design variables of the composite plate have on achieving an optimum minimum weight design?

For the optimization of the 3-phase laminate, five optimization problems were defined subjected to a frequency constraint, and design variables used were fibre volume content, CNT weight content, fibre stacking angle and thickness ratio of the individual layers of the composite plate. The main objective of this study was to achieve the optimal minimum weight design for the composite plate. This was achieved by introducing a design efficiency factor to assess the optimal minimum solution for each optimization problem. The design efficiency factor was successfully implemented by integrating the vibration of an unreinforced isotropic plate and the natural vibration of a 3-phase CNT/fibre reinforced nanocomposite plate. The reference plate formed the baseline for the weight and frequency parameters, which helped achieve non-dimensional quantities and the design efficiency factor.

- **(Problem 1)** The first problem comprised of the optimization of a 2-phase fibre reinforced laminate with fibre as the design variable. Numerical results for the optimal fibre angles were shown for different aspect ratios. For square plates (aspect ratio=1), the optimal fibre angle was 45° and for aspect ratios greater than 1, optimal fibre angle increased towards 90°. For the specified frequency constraint, the increase in aspect ratio of the laminate plate results in a decrease in the required stiffness, hence an increase in the optimal fibre angle for each layer. The reinforcement in the composite was optimized, giving higher amounts in the exterior layers and less concentrated amounts in the interior layers. This result correlated with results from past literature and promoted the use of effective material utilization in the composite.

The remaining optimization problems were formulated on the 3-phase CNT/fibre reinforced laminate.

- **(Problem 2)** In the second design problem, the effect of a 3-phase CNT/fibre reinforced laminate compared to a 2-phase laminate was presented. The 3-phase CNT/fibre reinforced laminate resulted in an improvement of the design efficiency factor and a better minimum weight design for the composite plate. The carbon nanotubes have shown to provide a better design efficiency whilst also giving more consistent results for all fibre angles, compared to the 2-phase fibre reinforced laminate.
- **(Problem 3)** In the third design optimization problem, two design variables (fibre and CNTs) were successfully modelled with the optimization algorithm together with the design constraints. Carbon nanotubes have shown to have a higher effect in providing stiffness to the plate due to its high tensile strength and low weight. Numerical results showed that by increasing the amount of CNTs in the laminate, this reduced the amount of fibre required, and simultaneously providing a more lightweight composite. This is a good result, but this can be very costly to incorporate high amounts of nanomaterials like CNTs in the laminate, thus assigning a limit for the amount of CNTs allowed in overall composite plate and also in a limit for each layer. For high frequency constraints, up to 2.4, a 51.2% reduction in the overall weight of the composite is achieved, compared to a reference unreinforced isotropic plate.

This optimized result highlights the innovation to this study by using nano reinforcement like CNTs and by modelling them using efficient optimization and material science techniques.

- **(Problem 4)** A further optimization problem involving the stacking sequence of the laminate was presented. An optimal minimum weight was obtained, with an improved design efficiency factor, using an angled ply stacking sequence compared to the traditional cross ply stacking sequence. For different aspect ratios, ranging from 1 to 2, an increase of 0.4% to 3.5% was noted. The benefit of using multiple design variables in the optimization was highlighted since more improved results were obtained.
- **(Problem 5)** Prior to the non-uniform reinforcement and uniform layer thickness optimization problems, an additional optimization problem involving non-uniform layer thickness was solved. Optimal values comprised of outer layers having a higher thickness to the inner layers. This was also subject to the reinforcement present in those layers which also contributed to the minimum weight design. The overall improvement of the non-dimensional weight was noted to be 52.7% for the composite plate with non-uniform reinforcement and non-uniform layer thickness. As mentioned previously, the added design variables allowed for a better design, where more parameters are being optimized in the composite, which resulted in a better design efficiency for the weight optimization problems.

5.2 Recommendations and future work

This study has provided a great understanding of structural engineering with composites. The implementation of CNTs in a 3-phase multiscale composite has highlighted its potential for further research in other applications which shall aim to fully utilise its incredible properties. In future efforts, this weight optimization approach can be extended using various other structural analysis methods such as buckling, bending, fractures and incorporating multiple boundary conditions to the composite plate. It would also be interesting and innovative to apply this research to a real-life scenario, possibly by means of designing an aircraft panel using nanomaterials and optimization, providing a lightweight and cost-effective design. The vibration problem of the composite plate can also be extended using with a functionally graded nanocomposite plate, incorporating optimization and multiple objective functions.

The use of CNTs and nanomaterials shows to be beneficial in most industries as research and development continues to improve. CNTs and the weight optimization problem with the composite plate and materials can be further researched and applied to the retrofitting of structures. The applications for it could apply to damaged structures, from seismic loadings, or even ancient structures which needs to be rehabilitated to increase its strength and durability. The further research on structures with nanocomposites and retrofitting would widen the opportunities of using CNTs and other nanomaterials in the civil engineering industry.

REFERENCES

Adali, S., Richter, A., Verijenko, V. E. & Summers, E. B. 1995. Optimal design of hybrid laminates with discrete ply angles for maximum buckling load and minimum cost. *Composite Structures,* 32**,** 409-415.

Adali, S. & Verijenko, V. E. 2001. Optimum stacking sequence design of symmetric hybrid laminates undergoing free vibrations. *Composite Structures,* 54**,** 131-138.

Ahmadi, M., Ansari, R. & Rouhi, H. 2017. Multi-scale bending, buckling and vibration analyses of carbon fiber/carbon nanotube-reinforced polymer nanocomposite plates with various shapes. *Physica E: Low-dimensional Systems and Nanostructures,* 93**,** 17-25.

Ahmadi, M., Ansari, R. & Rouhi, H. 2018. Free Vibration Analysis of Carbon Fiber-Carbon Nanotube-Polymer Matrix Composite Plates by a Finite Element-Based Multi-Scale Modeling Approach. *Journal of Multiscale Modelling,* 09**,** 1850002.

Akbulut, M. & Sonmez, F. O. 2011. Design optimization of laminated composites using a new variant of simulated annealing. *Computers & Structures,* 89**,** 1712-1724.

Aktemur, C. & Gusseinov, I. A Comparison of Sequential Quadratic Programming, Genetic Algorithm, Simulated Annealing, Particle Swarm Optimization and Hybrid Algorithm for the Design and Optimization of Golinsk‰ s Speed Reducer. 2017.

Almeida, F. S. & Awruch, A. M. 2009. Design optimization of composite laminated structures using genetic algorithms and finite element analysis. *Composite Structures,* 88**,** 443-454.

An, H., Chen, S. & Huang, H. 2019. Maximization of fundamental frequency and buckling load for the optimal stacking sequence design of laminated composite structures. *Proceedings of the Institution of Mechanical Engineers, Part L: Journal of Materials: Design and Applications,* 233**,** 1485-1499.

Assie, A. E., Kabeel, A. M. & Mahmoud, F. F. 2012. Optimum design of laminated composite plates under dynamic excitation. *Applied Mathematical Modelling,* 36**,** 668-682.

Aymerich, F. & Serra, M. 2008. Optimization of laminate stacking sequence for maximum buckling load using the ant colony optimization (ACO) metaheuristic. *Composites Part A: Applied Science and Manufacturing,* 39**,** 262-272.

Bader, B. W. 2009. 1.16 - Constrained and Unconstrained Optimization. *In:* BROWN, S. D., TAULER, R. & WALCZAK, B. (eds.) *Comprehensive Chemometrics.* Oxford: Elsevier.

Bekyarova, E., Thostenson, E. T., Yu, A., Kim, H., Gao, J., Tang, J., Hahn, H. T., Chou, T. W., Itkis, M. E. & Haddon, R. C. 2007. Multiscale carbon nanotube-carbon fiber reinforcement for advanced epoxy composites. *Langmuir : the ACS journal of surfaces and colloids,* 23**,** 3970-4.

Boggs, P. T. & Tolle, J. W. 1995. Sequential quadratic programming. *Acta numerica,* 4**,** 1-51.

Boyer, F., Olivier, P., Pons, F. & Cadaux, P. H. 2012. Mechanical and electrical behavior of a PEEK / Carbon Nanotubes composite. *ECCM 2012 - Composites at Venice, Proceedings of the 15th European Conference on Composite Materials*.

Bruntland, G. 1987. Report of the World Commission on environment and development; our common future, Bruntland report. *New York: UN Documents*.

Cantwell, W. J. & Morton, J. 1991. The impact resistance of composite materials — a review. *Composites,* 22**,** 347-362.

Cao, G. 2014. Atomistic Studies of Mechnaical Properties of Graphene. *Polymers,* 6**,** 2404-2432.

Cardozo, S., Gomes, H. M. & Awruch, A. M. 2011. Optimization of laminated composite plates and shells using genetic algorithms, neural networks and finite elements. *Latin American Journal of Solids and Structures,* 8**,** 413-427.

Dasgupta, A. 2018. Retrofitting of Concrete Structure with Fiber Reinforced Polymer. *International Journal,* 4**,** 42-49.

Demiroglu, S., Singaravelu, V., Seydibeyoğlu, M. Ö., Misra, M. & Mohanty, A. K. 2017. 13 - The use of nanotechnology for fibre-reinforced polymer composites. *In:* SEYDIBEYOĞLU, M. Ö., MOHANTY, A. K. & MISRA, M. (eds.) *Fiber Technology for Fiber-Reinforced Composites.* Woodhead Publishing.

Díez-Pascual, A. M., Naffakh, M., Marco, C., Gómez-Fatou, M. A. & Ellis, G. J. 2014. Multiscale fiber-reinforced thermoplastic composites incorporating carbon nanotubes: A review. *Current Opinion in Solid State & Materials Science,* 18**,** 62-80.

Duc, N. D., Lee, J., Nguyen-Thoi, T. & Thang, P. T. 2017. Static response and free vibration of functionally graded carbon nanotube-reinforced composite rectangular plates resting on Winkler–Pasternak elastic foundations. *Aerospace Science and Technology,* 68**,** 391-402.

Ebrahimi, F. & Dabbagh, A. 2019. An analytical solution for static stability of multi-scale hybrid nanocomposite plates. *Engineering with Computers*.

Ebrahimi, F. & Habibi, S. 2018. Nonlinear eccentric low-velocity impact response of a polymer-carbon nanotube-fiber multiscale nanocomposite plate resting on elastic foundations in hygrothermal environments. *Mechanics of Advanced Materials and Structures,* 25**,** 425-438.

Ehsani, A. & Rezaeepazhand, J. 2016. Stacking sequence optimization of laminated composite grid plates for maximum buckling load using genetic algorithm. *International Journal of Mechanical Sciences,* 119**,** 97-106.

Garg, B., Bisht, T. & Ling, Y.-C. J. M. 2014. Graphene-based nanomaterials as heterogeneous acid catalysts: a comprehensive perspective. 19**,** 14582-14614.

Gholami, R., Ansari, R. & Gholami, Y. 2018. Numerical study on the nonlinear resonant dynamics of carbon nanotube/fiber/polymer multiscale laminated composite rectangular plates with various boundary conditions. *Aerospace Science and Technology,* 78**,** 118-129.

Giambanco, G., Rizzo, S. & Spallino, R. 1999. *Optimal Design of Laminated Composite Plates*.

Gohardani, O., Elola, M. C. & Elizetxea, C. 2014. Potential and prospective implementation of carbon nanotubes on next generation aircraft and space vehicles: A review of current and expected applications in aerospace sciences. *Progress in Aerospace Sciences,* 70**,** 42-68.

Gong, G. 2018. Literature study of graphene modified polymeric composites.

Hansel, W. & Becker, W. 1999. Layerwise adaptive topology optimization of laminate structures. *Engineering Computations,* 16**,** 841-851.

Harris, B. 1991. A perspective view of composite materials development. *Materials & Design,* 12**,** 259-272.

Ho-Huu, V., Do-Thi, T. D., Dang-Trung, H., Vo-Duy, T. & Nguyen-Thoi, T. 2016. Optimization of laminated composite plates for maximizing buckling load using improved differential evolution and smoothed finite element method. *Composite Structures,* 146**,** 132-147.

Hossain, K. & Rameeja, S. 2015. Importance of Nanotechnology in Civil Engineering. *European Journal of Sustainable Development,* 4**,** 161-166.

Iijima, S. 1991. Helical microtubules of graphitic carbon. *Nature,* 354**,** 56-58.

Inam, F., Wong, D., Manabu, K. & Peijs, T. 2010. Multiscale Hybrid Micro-Nanocomposites Based on Carbon Nanotubes and Carbon Fibers. *Journal of Nanomaterials,* 2010.

Jamal-Omidi, M. & Shayanmehr, M. 2018. An experimental study on the nonlinear free vibration response of epoxy and carbon fiber-reinforced composite containing single-walled carbon nanotubes. *Journal of Vibration and Control,* 24**,** 4529-4540.

Jones, R. M. 1998. *Mechanics of composite materials,* CRC press.

Kalamkarov, A. L., Georgiades, A. V., Rokkam, S. K., Veedu, V. P. & Ghasemi-Nejhad, M. N. 2006. Analytical and numerical techniques to predict carbon nanotubes properties. *International Journal of Solids and Structures,* 43**,** 6832-6854.

Karakaya, Ş. & Soykasap, Ö. 2011. Natural frequency and buckling optimization of laminated hybrid composite plates using genetic algorithm and simulated annealing. *Struct. Multidiscip. Optim.,* 43**,** 61–72.

Kim, H., Abdala, A. A. & Macosko, C. W. 2010. Graphene/Polymer Nanocomposites. *Macromolecules,* 43**,** 6515-6530.

Leissa, A. W. & Narita, Y. 1989. Vibration studies for simply supported symmetrically laminated rectangular plates. *Composite Structures,* 12**,** 113-132.

Li, D., Muller, M. B., Giljer, S., Kaner, R. B. & Wallace, G. D. 2008. Processable aqueous dispersions of graphene nanosheets. *Nature Nanotechnology,* 3**,** 101-105.

Lin, C. C. & Yu, A. J. 1991. Optimum weight design of composite laminated plates. *Computers & Structures,* 38**,** 581-587.

Liu, D., Toropov, V. V., Barton, D. C. & Querin, O. M. 2015. Weight and mechanical performance optimization of blended composite wing panels using lamination parameters. *Structural and Multidisciplinary Optimization,* 52**,** 549-562.

Liu, Q. & Paavola, J. 2016. Lightweight design of composite laminated structures with frequency constraint. *Composite Structures,* 156**,** 356-360.

Logan, D. L. 2007. *First Course in the Finite Element Method,* Thomson.

Lopez, R. H., Luersen, M. A. & Cursi, E. S. 2009. Optimization of laminated composites considering different failure criteria. *Composites Part B: Engineering,* 40**,** 731-740.

Maalawi, K. 2018. An Introduction to the Optimization of Composite Structures.

Madeo, A. 2015. 2 - Fibrous Composite Reinforcements. *In:* MADEO, A. (ed.) *Generalized Continuum Mechanics and Engineering Applications.* Elsevier.

Mccarthy, C. & Vaughan, T. 2015. 14 - Micromechanical failure analysis of advanced composite materials. *In:* CAMANHO, P. P. & HALLETT, S. R. (eds.) *Numerical Modelling of Failure in Advanced Composite Materials.* Woodhead Publishing.

Mehar, K., Panda, S. K. & Mahapatra, T. R. 2017. Theoretical and experimental investigation of vibration characteristic of carbon nanotube reinforced polymer composite structure. *International Journal of Mechanical Sciences,* 133**,** 319-329.

Morshed, M. J. & Asgharpour, A. 2014. Hybrid imperialist competitive-sequential quadratic programming (HIC-SQP) algorithm for solving economic load dispatch with incorporating stochastic wind power: A comparative study on heuristic optimization techniques. *Energy Conversion and Management,* 84**,** 30-40.

Nagavally, R. R. 2017. Composite Materials- History, Types, Fabrication Techniques, Advantages and Applications. *International Journal of Mecahnical and Production Engineering,* 5**,** 82-87.

Narita, Y. 2003. Layerwise optimization for the maximum fundamental frequency of laminated composite plates. *Journal of Sound and Vibration,* 263**,** 1005-1016.

Nasrollahzadeh, M., Sajadi, S. M., Sajjadi, M. & Issaabadi, Z. 2019. Chapter 4 - Applications of Nanotechnology in Daily Life. *In:* NASROLLAHZADEH, M., SAJADI, S. M., SAJJADI, M., ISSAABADI, Z. & ATAROD, M. (eds.) *Interface Science and Technology.* Elsevier.

Nikbakt, S., Kamarian, S. & Shakeri, M. 2018. A review on optimization of composite structures Part I: Laminated composites. *Composite Structures,* 195**,** 158-185.

Park, C. H., Lee, W. I., Han, W. S. & Vautrin, A. 2003. Weight minimization of composite laminated plates with multiple constraints. *Composites Science and Technology,* 63**,** 1015-1026.

Park, S.-J. & Seo, M.-K. 2011. Chapter 8 - Composite Characterization. *In:* PARK, S.-J. & SEO, M.-K. (eds.) *Interface Science and Technology.* Elsevier.

Pelletier, J. L. & Vel, S. S. 2006. Multi-objective optimization of fiber reinforced composite laminates for strength, stiffness and minimal mass. *Computers & Structures,* 84**,** 2065-2080.

Prashanth, S., Subbaya, K., Nithin, K. & Sachhidananda, S. 2017. Fiber Reinforced Composites-A Review. *Journal of Materials Sciences and Engineering,* 6.

Qiu, H. & Yang, J. 2017. Chapter 2 - Structure and Properties of Carbon Nanotubes. *In:* PENG, H., LI, Q. & CHEN, T. (eds.) *Industrial Applications of Carbon Nanotubes.* Boston: Elsevier.

Rafiee, M., Nitzsche, F. & Labrosse, M. R. 2018. Cross-Sectional Design and Analysis of Multiscale Carbon Nanotubes-Reinforced Composite Beams and Blades. *International Journal of Applied Mechanics,* 10**,** 1850032.

Rafiee, R. & Eskandariyun, A. 2019. Estimating Young's modulus of graphene/polymer composites using stochastic multi-scale modeling. *Composites Part B: Engineering,* 173**,** 106842.

Rajabpour, M., Hemmatian, H. & Fereidoon, A. 2011. *Investigation of length and chirality effects on Young's modulus of heterojunction nanotube with FEM.*

Rao, N. V., Rajasekhar, M., Vijayalakshmi, K. & Vamshykrishna, M. 2015. The Future of Civil Engineering with the Influence and Impact of Nanotechnology on Properties of Materials. *Procedia Materials Science,* 10**,** 111-115.

Reddy, J. N. 2003. *Mechanics of laminated composite plates and shells: theory and analysis,* CRC press.

Sadd, M. H. 2014. Chapter 15 - Micromechanics Applications. *In:* SADD, M. H. (ed.) *Elasticity (Third Edition).* Boston: Academic Press.

Salamanca-Buentello, F., Persad, D. L., Court, E. B., Martin, D. K., Daar, A. S. & Singer, P. A. 2005. Nanotechnology and the Developing World. *PLOS Medicine,* 2**,** e97.

Sanchez, A., Román-Velázquez, C. & Noguez, C. 2005. Optical circular dichroism of single-wall carbon nanotubes. *Physical Review B,* 73**,** 045401.

Sanchez, F. & Sobolev, K. 2010. Nanotechnology in concrete – A review. *Construction and Building Materials,* 24**,** 2060-2071.

Seidi, J. & Kamarian, S. 2017. Free vibrations of non-uniform CNT/fiber/polymer nanocomposite beams. *Curved and Layered Structures* [Online], 4.

Shin, D. K., Gu¨Rdal, Z. & Griffin, O. H., Jr. 1991. Minimum Weight Design of Laminated Composite Plates for Postbuckling Performance. *Applied Mechanics Reviews,* 44**,** S219-S231.

Tserpes, K. I. & Silvestre, N. 2014. *Modeling of carbon nanotubes, graphene and their composites*, Springer.

United Nations. Economic Commission for Africa. 2020. Towards an African nanotechnology future: trends, impacts and opportunities.

Uppal, R. 2020. *Carbon Nanotubes(CNT) for Aerospace applications including composites for lightweight structural components, aircraft braking systems, electromagnetic interference (EMI), radio frequency interference (RFI), electrostatic discharge (ESD), and de-icing* [Online]. International Defense Security & Technology Inc. Available: https://idstch.com/military/air/carbon-nanotubes-for-aerospace-applications/ [Accessed 20 December 2020].

Velmurugan, R. & Manikandan, V. 2005. Mechanical properties of glass/palmyra fiber waste sandwich composites. *Indian Journal of Engineering and Materials Science,* 12**,** 563-570.

Vidu, R., Rahman, M., Mahmoudi, M., Enachescu, M., Poteca, T. & Opris, I. 2014. Nanostructures: A Platform for Brain Repair and Augmentation. *Frontiers in systems neuroscience,* 8**,** 91.

Vo-Duy, T., Ho-Huu, V., Do-Thi, T. D., Dang-Trung, H. & Nguyen-Thoi, T. 2017. A global numerical approach for lightweight design optimization of laminated composite plates subjected to frequency constraints. *Composite Structures,* 159**,** 646-655.

Volterra, V. Sur l'équilibre des corps élastiques multiplement connexes. Annales scientifiques de l'École normale supérieure, 1907. 401-517.

Wang, C. Y. & Wang, C. 2013. *Structural vibration: exact solutions for strings, membranes, beams, and plates,* CRC Press.

Wang, J. & Blau, W. 2007. *Carbon nanotubes for optical limiting: The nonlinear optical properties of dispersions of single-walled carbon nanotubes make them attractive for use in laser-protective eyewear* [Online]. Spie.org. Available: https://spie.org/news/0916-carbon-nanotubes-for-optical-limiting?SSO=1 [Accessed 08 December 2020].

Wang, X., Wang, Y. & Xu, S. 2012. DSC analysis of a simply supported anisotropic rectangular plate. *Composite Structures,* 94**,** 2576-2584.

Wu, C. & Viquerat, A. 2017. Natural frequency optimization of braided bistable carbon/epoxy tubes: Analysis of braid angles and stacking sequences. *Composite Structures,* 159**,** 528-537.

Yang, X.-S. 2013. 1 - Optimization and Metaheuristic Algorithms in Engineering. *In:* YANG, X.-S., GANDOMI, A. H., TALATAHARI, S. & ALAVI, A. H. (eds.) *Metaheuristics in Water, Geotechnical and Transport Engineering.* Oxford: Elsevier.

Yang, Y., Boom, R., Irion, B., Van Heerden, D.-J., Kuiper, P. & De Wit, H. 2012. Recycling of composite materials. *Chemical Engineering and Processing: Process Intensification,* 51**,** 53-68.

Zhang, S., Wang, H., Wang, G. & Jiang, Z. 2012. Material with high dielectric constant, low dielectric loss, and good mechanical and thermal properties produced using multi-wall carbon nanotubes wrapped with poly(ether sulphone) in a poly(ether ether ketone) matrix. *Applied Physics Letters,* 101.

APPENDIX A - EFFECTIVE PROPERTIES

Table A-0-1: Effective layer material properties

Wt % CNT	Vol % Fibre	E_1	E_2	ν	G	Density
0	0	3.50E+09	3.50E+09	0.35	1.30E+09	1200.00
0.00125	0.1	3.76E+09	3.76E+09	0.3499	1.39E+09	1200.20
0	0.1	1.04E+10	4.21E+09	0.335	1.43E+09	1320.00
0.00125	0.1	1.06E+10	4.51E+09	0.3349	1.54E+09	1320.20
0	0.2	1.73E+10	4.78E+09	0.32	1.60E+09	1440.00
0.00125	0.2	1.75E+10	5.13E+09	0.3199	1.72E+09	1440.20
0.002	0.2	1.76E+10	5.33E+09	0.3199	1.79E+09	1440.30
0.00125	0.25	2.09E+10	5.47E+09	0.3124	1.83E+09	1500.20
0	0.3	2.42E+10	5.45E+09	0.305	1.82E+09	1560.00
0.00125	0.3	2.44E+10	5.85E+09	0.3049	1.95E+09	1560.20
0.002	0.3	2.45E+10	6.08E+09	0.3049	2.03E+09	1560.30
0.00125	0.35	2.78E+10	6.27E+09	0.2974	2.09E+09	1620.20
0.01	0.3	2.56E+10	8.54E+09	0.305	2.89E+09	1561.30
0.0125	0.3	2.60E+10	9.29E+09	0.3044	3.15E+09	1561.70
0.02	0.3	2.71E+10	1.15E+10	0.304	3.93E+09	1562.70
0.03	0.3	2.86E+10	1.44E+10	0.3035	4.96E+09	1564.00
0.04	0.3	3.01E+10	1.71E+10	0.303	5.97E+09	1565.40

APPENDIX B – ANSYS RESULTS

Table B-0-1: Optimal weight quantities determined using ANSYS

CNT (: , 8)	Vf	W_L (kg)	h-ref	W_0-ref (kg)	W_nondim
0.00125	0.2/0/0/0	12.60200	0.01484	17.81000	0.71000
0.00125	0.25/0/0/0.2	13.35200	0.01527	18.32000	0.73000
0.00125	0.25/0/0/0.1	13.05200	0.01540	18.49000	0.71000
0.00125	0.2/0.1/0/0	12.90200	0.01544	18.52000	0.70000
0.00125	0.25/0/0/0	12.75200	0.01554	18.65000	0.68000
0.00125	0.25/0/0.1/0	13.05200	0.01563	18.76000	0.70000
0.00125	0.25/0/0.2/0	13.35200	0.01572	18.87000	0.71000
0.00125	0.2/0.2/0/0	13.20200	0.01599	19.18000	0.69000
0.00125	0.2/0.2/0.1/0	13.50200	0.01605	19.27000	0.70000
0.00125	0.25/0.1/0/0	13.05200	0.01608	19.29000	0.68000
0.00125	0.3/0/0/0	12.90200	0.01620	19.44000	0.66000
0.00125	0.35/0/0/0.2	13.65200	0.01653	19.83000	0.69000
0.00125	0.25/0.2/0/0	13.35200	0.01658	19.89000	0.67000
0.00125	0.35/0/0/0.1	13.35200	0.01668	20.01000	0.67000
0.00125	0.3/0.1/0/0	13.20200	0.01668	20.02000	0.66000
0.00125	0.35/0/0/0	13.05200	0.01683	20.20000	0.65000
0.00125	0.35/0/0.1/0	13.35200	0.01688	20.25000	0.66000
0.00125	0.35/0/0.2/0	13.65200	0.01693	20.31000	0.67000
0.00125	0.3/0.2/0/0	13.50200	0.01714	20.57000	0.66000
0.00125	0.3/0.2/0.1/0	15.60200	0.01717	20.61000	0.76000
0.00125	0.35/0.1/0/0	13.35200	0.01727	20.72000	0.64000

Table B-0-2: Optimal Frequency quantities determined using ANSYS

CNT (: , 8)	Vf	Frequency (Hz)	ω_1 (rad/s)	f_nondim
0.00125	0.2/0/0/0	24.53900	154.18308	1.48897
0.00125	0.25/0/0/0.2	25.24800	158.63786	1.53199
0.00125	0.25/0/0/0.1	25.47000	160.03273	1.54546
0.00125	0.2/0.1/0/0	25.52200	160.35946	1.54862
0.00125	0.25/0/0/0	25.70100	161.48415	1.55948
0.00125	0.25/0/0.1/0	25.84800	162.40777	1.56840
0.00125	0.25/0/0.2/0	25.99600	163.33769	1.57738
0.00125	0.2/0.2/0/0	26.43100	166.07087	1.60378
0.00125	0.2/0.2/0.1/0	26.54500	166.78715	1.61069
0.00125	0.25/0.1/0/0	26.58200	167.01963	1.61294
0.00125	0.3/0/0/0	26.79100	168.33282	1.62562
0.00125	0.35/0/0/0.2	27.32900	171.71317	1.65827
0.00125	0.25/0.2/0/0	27.40600	172.19698	1.66294
0.00125	0.35/0/0/0.1	27.57500	173.25883	1.67319
0.00125	0.3/0.1/0/0	27.58600	173.32795	1.67386
0.00125	0.35/0/0/0	27.83100	174.86733	1.68873
0.00125	0.35/0/0.1/0	27.90600	175.33857	1.69328
0.00125	0.35/0/0.2/0	27.98700	175.84751	1.69819
0.00125	0.3/0.2/0/0	28.33900	178.05919	1.71955
0.00125	0.3/0.2/0.1/0	28.39400	178.40476	1.72289
0.00125	0.35/0.1/0/0	28.55400	179.41007	1.73260